NASA Contractor Report 2939

Kinetics of Pack Aluminization of Nickel

L. L. Seigle, B. K. Gupta,
R. Shankar, and A. K. Sarkhel

CONTRACT NGR-33-015-160
JANUARY 1978

NASA

NASA Contractor Report 2939

Kinetics of Pack Aluminization of Nickel

L. L. Seigle, B. K. Gupta,
R. Shankar, and A. K. Sarkhel
State University of New York
Stony Brook, New York

Prepared for
Lewis Research Center
under Contract NGR-33-015-160

National Aeronautics
and Space Administration

**Scientific and Technical
Information Office**

1978

FOREWORD

This is the final report of work conducted in the laboratories of the Materials Science Department, State University of New York, Stony Brook, New York, during the period June 1, 1972, to September 30, 1976. Participants in the project included the project director, Professor Leslie L. Seigle, and research assistants B.K. Gupta, A.K. Sarkhel, S. Shankar, and R. Sivakumar. The report is based on the Ph.D. theses of these students, particularly that of B.K. Gupta. Dr. S.R. Levine of the NASA Lewis Research Center, who served as project manager, is thanked for furnishing the Ni-Al alloys used in the diffusion studies and also for his suggestions concerning the gas diffusion rate constant calculations. Contribution of some Ni-Al alloys by the Materials Engineering and Research Laboratory of the Pratt & Whitney Division of United Technologies Corporation is gratefully acknowledged.

TABLE OF CONTENTS

SUMMARY

A study has been made of the kinetics of pack aluminization of unalloyed nickel in packs of varying aluminum activity with various halide activators over the temperature range 800-1093°C. The activators investigated included AlF_3, NaF, NaCl and NaI. The aluminum activity of the packs was varied by varying the ratio of Al to Ni in the pack powders from 45 a/o Al/65 a/o Ni to 100 a/o Al. The surface compositions of the coatings were obtained as functions of time, temperature and pack composition by electron microprobe analysis, in order to establish the boundary conditions for diffusion in the system. In addition, weight gains of the specimens were measured and studies of the structure of the packs were carried out to further clarify the mechanism of aluminization.

In order to correlate rates of coating formation with diffusivities in the solid, the variation of the interdiffusion coefficient, $\tilde{D}$, with composition in the δ(NiAl) phase of the Al-Ni system was determined over the range 850-1150°C. Additional diffusivity data were also obtained for other phases in this system.

The above studies indicated that in packs activated with AlF_3, NaF and NaCl the Al concentration of the surface of the coating reached a steady value in a short period of time, which remained almost constant, under most circumstances, for the duration of the coating process. This surface concentration, however, was not identical with the pack Al concentration but fell below the pack concentration by various amounts, depending primarily upon the pack Al activity and type of activator used. The square of the weight gain of the specimen during coating was usually found to vary linearly with time. Highest surface Al concentrations and coating rates were obtained with the fluoride activators, followed by the chloride and then the iodide. The performance of the iodide activator was much poorer than the fluoride and chloride activators.

Examination of the structure of pure Al packs after coating revealed the presence of an Al-depleted zone in the pack adjacent to the coated specimen. The weight of Al lost from this depleted zone, calculated from its dimensions, agreed closely with the measured weight gain of Al by the specimen. This result is in agreement with Levine and Caves model for the kinetics of Al transport in the pack by diffusion of aluminum halide vapors. By combining Levine and Caves model for gaseous diffusion in the pack with calculations of rates of solid diffusion in the coating a more complete theory for the kinetics of pack aluminization was formulated. Using available thermodynamic and diffusivity data theoretical rates of aluminization of Ni were calculated for packs of varying Al activity, type of activator and operating temperature. Theoretical predictions were in reasonably good agreement with experimental results and it is felt that the theory formulated supplies a good basis for estimating the influence of processing parameters upon rates of aluminization under many conditions.

INTRODUCTION

Aluminide coatings are frequently used to improve the oxidation - corrosion resistance and extend the life of superalloy blades and vanes at high temperatures in gas turbines. Such coatings may be applied by a variety of methods but the pack - "cementation" method has proven to be a simple and useful technique for depositing aluminide coatings on superalloys and is widely used commercially. While there is a fairly extensive literature on pack aluminizing, our understanding of this process is still far from complete. An examination of the aluminizing of nickel-base superalloys and unalloyed nickel by Goward, Boone and Giggins (ref. 1) and Goward and Boone (ref. 2) led to the conclusion that Ni_2Al_3 is the main coating phase formed in high aluminum activity packs at low temperatures, while NiAl is the principal phase occurring in coatings formed in low aluminum activity packs at high temperatures. An analysis of the thermochemical fundamentals of pack-aluminizing was carried out by Walsh (ref. 3) leading to some qualitative conclusions about pack design. Brill-Edwards and Epner (ref. 4) interpreted discontinuities in coatings formed on superalloys in terms of various material transfer mechanisms. By far the most definitive study of the pack-aluminization process to date was carried out by Levine and Caves (ref. 5). These workers investigated the effects of pack variables on the formation of coatings on the nickel-base superalloy IN-100 and analyzed their results in terms of a theoretical model for gaseous diffusion in the pack. They concluded that diffusion in the solid controlled the rate of coating formation in packs activated with NaF, NaCl and NH_4F, while gaseous diffusion was controlling in packs activated with other sodium and ammonium halides.

While various aspects of the aluminization process have been clarified by these investigators, a rigorous and complete analysis has not yet been carried out. In the above studies, for example, it is clear that the surface of the coating under formation was not in equilibrium with the pack. It must be questioned, therefore, whether diffusion in the solid was at any time entirely rate controlling. Constancy of composition at the surface of the coating, a critical condition for diffusion control, was not demonstrated. The relationships between rates of coating formation and solid state diffusivity values in the coating-substrate systems could not be evaluated with precision. It appeared, therefore, that our understanding of the kinetics of pack-aluminization was still incomplete and further work was required to clarify the details of this process.

The purpose of this study was to develop a fuller understanding of the factors controlling the kinetics of the pack-aluminization process and in particular to correlate rates of coating formation and coating structures with the basic diffusivity parameters of the solid. To achieve this aim a study was conducted of the aluminization of unalloyed nickel from packs of controlled aluminum activity over a range of

operating conditions. The boundary conditions for diffusion in the solid were investigated by determining the time variation of the composition of the surface of the coating through microprobe analysis. A rigorous calculation of rates of coating formation was carried out, using diffusivity data available for the Al-Ni system, and by combining these results with Levine and Caves model for gaseous diffusion in the pack, a more complete description of the kinetics of the pack-aluminization process was obtained.

EXPERIMENTAL PROCEDURES

Pack-Aluminizing

Pack-aluminizing was carried out in cylindrical iron retorts, 3.4 cm. I.D. x 12.5 cm. long, heated in a resistance furnace fitted with an Inconel tube of 5 cm. I.D. The retorts were closed with a slip-fitted iron cap (Fig. 1) and thus were not tightly sealed. Most retorts were fitted with an impervious alumina liner to minimize reaction with the retort wall. The packs consisted of powder mixtures of 99.5% pure Al, Ni, or Al-Ni alloy, various activators, and Al_2O_3 as inert filler. The average particle size of the Al powder was 15-17 μm, that of the Ni powder 4-7 μm and of the Al_2O_3 powder 5 μm. Activators included chemically pure AlF_3, NaF, NaCl and NaI which were ground in a mortar and pestle before being added to the pack. Cylinders of commercial grade Ni(99.4 w/o Ni) 1 cm diameter and 1 cm. long were used as the specimens to be coated. All aluminizing runs were carried out in an atmosphere of prepurified hydrogen.

Prior to use in the coating experiments the retorts were conditioned by heating for several days with a pack of the same composition in order to aluminize the interior walls. When alloy packs were used (those containing both Ni and Al powders) the pack was pretreated for 10-20 hours at 1093°C to ensure complete reaction between the Ni and Al before use in the coating experiments. The ratio of metal to non-metal in the pack was varied according to pack Al/Ni ratio. For packs with Al/Ni ratios less than 70 a/o Al, the packs usually contained 48 w/o Al + Ni, 48 w/o Al_2O_3 and 4% activator. The metal to non-metal ratio in packs with higher Al/Ni ratios was decreased in order to avoid problems with melting in the pack, reaching a minimum of a few w/o in pure Al packs. A steady flow of hydrogen (about .05 cm^3/sec) was maintained during the coating operation. Coating temperatures ranged from 800 - 1095°C and times from 1-70 hours. The Ni specimens were prepared by polishing with fine emery paper and degreasing in acetone prior to coating. Normally two or three specimens were stacked at equal intervals in the center of the pack. After coating the samples were cleaned by brushing with a stiff nylon brush and by ultrasonic treatment in acetone. The weight gains of the samples were measured. Some samples were prepared for metallographic examination and

surface composition analysis.

Surface Composition Analysis - The surface composition of the coating was obtained by microprobe analysis at 5-10 locations in grain interiors on the center portion of the end surfaces of the Ni cylinders. The ARL-AMX electron microprobe was operated at 15 kv filament voltage and 0.015 μA sample current on brass. Intensities of Ni-Kα and Al-Kα lines were evaluated with respect to digitally integrated probe current instead of time, in order to minimize errors due to instability and drift of the current. Raw intensity counts were corrected and converted to compositions using Colby's MAGIC program (ref. 6). Two samples of homogeneous Ni-Al alloys were used as standards. One contained 68.3 ± 0.2 w/o Ni and 31.1 ± 0.2 w/o Al by wet chemical analysis. The other contained 13.5 ± 0.2 w/o Al.

RESULTS

Kinetics of Aluminizing in Al-Ni Alloy Packs

The variations of the surface composition and square of the specific weight gain vs. time of nickel specimens aluminized at 1093°C in packs containing Al and Ni in various proportions are shown in Figs. 2-5. It may be seen that within a short period of time (time was measured from the moment that the retort was pushed from a cold end into the hot zone of the furnace) the surface composition reached a steady value which remained almost constant for times exceeding 20 hours. The square of the specific weight gain varied linearly with time during this period, except for a short initial period of slow growth which may in most cases be identified with the time for the retort to come to temperature. The observed kinetics, therefore, to a good approximation follow the laws of diffusion from a surface of constant composition into an infinitely extended medium.*

While the surface Al concentrations observed were practically time invariant, they did not correspond exactly to the pack Al concentrations, but fell below these to varying degrees. The relation between the Al concentration at the surface of the coating and that in the pack is given in Fig. 6. The heavy line in this figure gives the relationship between surface concentration and pack concentration to be expected if the surface of the coating were in equilibrium with the pack. Horizontal portions of this line correspond to two-phase regions in the Al-Ni phase equilibrium diagram. Surface compositions of specimens coated in packs

*Since the thickness of the coatings was ~ 10^{-2} cm while the specimen diameter was 1 cm., the diffusion problem can be treated as virtually linear diffusion into an infinitely extended medium.

activated with AlF_3 and NaF fall close together at values 5-7 a/o below the equilibrium values. Surface compositions in packs activated with NaCl fall slightly below those obtained in fluoride activated packs, and surface compositions obtained in NaI activated packs are substantially below the nominal pack compositions. Differences among the activators are particularly clearly illustrated in the results obtained with packs using commercial prealloyed 70 a/o Al 30 a/o Ni (Raney alloy) shown in Fig. 5 in which it may be seen that the highest surface compositions and most rapid weight gains were obtained with AlF_3 and NaF as activators followed by NaCl and NaI.

Since it was expected that losses of Al by diffusion into the specimens, retort walls and possible losses through the vapor phase would bring the actual Al/Ni ratios of the packs below the nominal ratios, an effort was made to determine the actual ratios by microprobe analysis of the pack metallic constituents at various stages of the coating process. In order to accomplish this, portions of the pack were impregnated, in situ, with catalytically hardening epoxy resin. These specimens were then prepared for examination by standard metallographic procedures. Fig. 7 reveals the distribution of alloy particles in AlF_3 activated packs of varying Al/Ni ratios after 10 hrs. at 1093°C. Since only Al is transferred through the vapor phase during heat treatment, the particle distribution reflects the original distribution of the Ni particles. As the Al/Ni ratio increases, both the interparticle spacing and the particle size increase as expected.

The composition of individual particles was determined by microprobe analyses. For the sake of accuracy only patches exceeding 5 μm in diameter in the cross sections were subject to analysis. The average compositions are given in Table 1 and Fig. 8. It may be seen that there is a loss of 2-3 a/o Al from the pack during pretreatment and another loss of about 1 a/o Al during coating so that the actual pack composition is 3-4 a/o Al below the nominal composition.

However this loss of Al is still not large enough to account for the observed divergence of the composition of the specimen surface from that of the pack and it appears that a small but appreciable difference exists between the Ni:Al ratio in the pack and that at the specimen surface during the coating process in these packs.

Kinetics of Aluminizing in Unalloyed Al Packs

The variation of surface composition and square of specific weight gain vs. time of specimens aluminized in packs containing unalloyed Al is shown in Figs. 9-12. At 1000 and 1093°C in packs charged with 4 w/o Al and 4 w/o activator (Figs. 11 and 12), except for an initial transient period surface compositions were again time invariant within a percent or two and the plots of specific weight gain squared vs. time approximately linear. (The lines for AlF_3 and NaF in Fig. 12 are shown dotted and no surface composition data are given because the specimen surfaces

melted during the coating process in these packs at 1093°C. Furthermore irregular surfaces on the specimens treated in NaI activated packs at 1000°C are responsible for the wide scatter in measured surface compositions shown in Fig. 11.) At 900°C (Fig. 10) surface compositions were once more substantially time invariant but the w^2 vs. time relationships departed from linearity to a greater degree than previously observed. The curves exhibit a period of initially low rate constant which is more extended than can be accounted for by time required to reach temperature alone. At 800°C, also, (Fig. 9) the coating rates did not strictly follow a linear w^2 vs. t relationship and a more appreciable change of surface composition with time is observed. In case of AlF_3 activated packs these discrepancies seemed to be associated with the condensation of AlF_3 at the specimen surface. A tightly adherent layer of pack material was observed on many of the surfaces after coating at 800 and 900°C, as shown in Fig. 13. X-ray image scanning carried out with the microprobe proved that this layer contained a high percentage of fluorine. On the other hand, specimens coated at higher temperatures were relatively free of adhering pack material. As discussed later, condensation of the activator at the coating surface is expected to occur and it is easily visualized that the condensate might fill the pores in these packs and help to create an impervious layer which impedes further transport of Al to the specimen surface. The effect of varying the amount of AlF_3 in packs operated at 900°C tends to bear out this explanation since it will be observed in Fig. 14 that with 1 w/o AlF_3 normal kinetics were obtained in 4 w/o pure Al packs at 900°C while the use of 6 w/o AlF_3 led to a drastic reduction in the rate of aluminization. A tightly adherent layer of pack was observed on the surface of the specimens coated in the 6 w/o AlF_3 pack, but not on the specimens in the 1 and 4 w/o AlF_3 packs (Fig. 15). However, a similar condensation of activator was not obtained with the other activators and all details of this phenomenon are not yet clearly understood.

Figs. 9-12 show clearly the order of effectiveness of the various activators, since without exception, AlF_3 yielded the highest coating rates, followed by NaF, NaCl and NaI in that order. Data for NaI were not included in Figs. 9 and 10 because the occurrence of very poor surfaces on specimens coated in packs with this activator at 800 and 900°C led to difficulties in measuring the surface compositions and weight gains. Data for NaCl are absent from Fig. 9 for the same reason.

It will be observed that the highest value of surface Al concentration is obtained in AlF_3 activated packs with successively lower values appearing in NaF, NaCl and NaI activated packs. The surface Al concentrations obtained with various activators and at various temperatures range for the most part from about 36-62 a/o Al corresponding to compositions in the NiAl and Ni_2Al_3 phase fields. However the evidence for liquefaction at 1093°C (Fig. 16) suggests that even higher surface Al concentrations were produced in AlF_3 and NaF activated, pure Al packs at this temperature.

Macrophotographs of impregnated and sectioned 4 w/o Al packs with various activators after coating at 1000 and 1093°C are given in Fig. 17 and 18, showing the regions adjacent to the cavities originally containing the Ni specimens. The light colored ring around the cavities represents zones depleted in Al.* The edge of one of these zones is shown at higher magnification in Fig. 18, and it may be seen that Al particles are present in the undepleted pack, to the left, while no such particles are evident in the depleted zone, to the right. The amount of Al lost from the depleted zone, calculated by multiplying the volume of this zone (obtained from the dimension of the ring) by the original pack Al density is compared in Table II with the measured weight gain of the coated specimen. It may be seen that almost all (average 96%) of the Al which has entered the coating has come from the depleted zone.

DISCUSSION OF RESULTS

The presence of a depleted zone adjacent to the coating surface and the fact that the Al gained by the specimen comes almost entirely from this zone, confirms the essential validity of the gaseous diffusion model of Levine and Caves (ref. 5) for transport of Al in the pack. In this model it is assumed that Al is transported from the pack to the specimen surface by diffusion of gaseous aluminum halides through a depleted zone of steadily increasing width. Under the assumption that the Al activity at the coating surface is a constant, a parabolic relationship is obtained between the amount of Al transferred, W_g (gms/cm^2), and time, t (seconds),

$$W_g^2 = K_g\, t \qquad (1)$$

where

$$K_g = \frac{2\rho\varepsilon M}{1RT} \sum_i \sigma_i D_i (P_i - P_i') \qquad (2)$$

In these equations ρ = pack Al density (gms/cm^2), M = gram atomic weight of Al, ε and 1 are correction factors for the density and tortuosity of the porous pack, D is the gas interdiffusion coefficient, P and P' are the equilibrium vapor pressures in the pack and at the coating surface, resp. and σ_i is a stoichiometric factor introduced to allow for the fact that some of the Al transferred to the surface may condense in the form of

*The fact that the undepleted pack appears gray in color while the depleted zone is almost white may be attributed to discoloration of the Al_2O_3 in the presence of a high Al activity. Loss of Al to the retort wall has evidently also occurred at the circumference of the pack.

aluminum halide rather than entering the specimen. The summation is carried over all diffusing species.

The experimental data obtained in the present work indicate that the surface composition (and therefore the surface Al activity) of the coating is often nearly time independent, as assumed by Levine and Caves, but it does not have a fixed value. The surface Al concentration varies with variations in pack operating parameters such as Al content and type of activator. Specification of this unknown surface concentration is essential to completely define the kinetics of the coating process.

If the surface concentration is time invariant, its value may be calculated from a knowledge of the solid as well as gas diffusion constants of the system (ref. 7, 8). This calculation is based on the fact that in the presence of a constant surface composition, assuming unidirectional diffusion into an infinitely extended medium, the rate of diffusion in the solid is also governed by a parabolic relationship,

$$W_s^2 = K_s\ t \tag{3}$$

where W_s^2 represents the amount of Al which has diffused into the solid in time, t. In this expression K_s is the parabolic rate constant for diffusion in the solid, which depends upon the phase boundary concentrations and diffusivity constants of the phases appearing in the coating, as well as the Al concentration at the surface. In order for a steady state to exist at the surface it is necessary that

$$W_s^2 = W_g^2 \tag{4}$$

and therefore,

$$K_s = K_g \tag{5}$$

If both K_s and K_g can be calculated as functions of surface concentration, for a given set of pack operating conditions, the value of concentration at which the two rate constants become equal can be obtained and thus the unknown surface composition defined.

Sufficient thermodynamic and diffusivity data exist to allow such calculations to be carried out for the aluminization of unalloyed Ni. Details are given in App. A and B. The variations of K_g and K_s with surface composition in packs with 4 w/o Al, for various activators at various temperatures, are shown in Figs. 19-22. The points of intersecting of the K_g and K_s curves give the predicted surface compositions and rate constants for the various packs and these predicted values are compared with experimental values in Tables III and IV. It may be seen

that theory and experiment are in complete agreement with respect to the order of efficiency of the activators. The most effective activator is AlF_3, followed, in order, by NaF, NaCl and NaI. The theory comes close to predicting the surface compositions and parabolic rate constants for packs activated with AlF_3, NaF, and NaCl. The predicted surface Al concentrations are 1-2 % higher than the observed concentrations for packs activated with AlF_3 and NaF, while they are slightly lower than the observed concentrations for packs activated with NaCl. Predicted rate constants fall within the range of the experimental values for AlF_3, are slightly below range for NaF, and low by a factor of 2-3 for NaCl. (Due to the fact that the w^2 vs. t curves were not precisely linear, upper and lower limits for the experimental constants are given, rather than single values.).

The few experimental results for NaI depart significantly from the theoretical values. Both the surface composition and K values observed are far lower than predicted by theory. As previously mentioned, very poor surfaces and irregular layer growth were frequently encountered on specimens coated in NaI activated packs. Porous coatings were often observed. Microstructures of coatings obtained in iodide and fluoride activated packs are compared in Fig. 3. The reason for these anomalies is not understood, but slowness of reactions at the coating surface is a possible factor.

Although no experiments were carried out using NH_4Cl activated packs, theoretical K_g curves for this activator are also shown in Figs. 19-22. In distinction to the other activators considered, no condensed phase is present in NH_4Cl activated packs at elevated temperatures. The absence of a condensed phase leads to a considerably different variation of K_g with temperature for NH_4Cl than for the other activators. K_g for this activator increases much more slowly with temperature than for the others. Also, for this activator K_g is sensitive to the percentage of activator added to the pack, whereas K_g for the others is insensitive to the percentage added (above a certain very small value). Therefore, there are significant differences between the operating characteristics of "volatile" activators, such as NH_4Cl, with which no condensed phase appears in the pack and "non-volatile" activators, such as AlF_3 and the sodium halides, with which a condensed phase is present in the pack. These differences were pointed out by Walsh (ref. 3) and are explained more fully in Appendix A.

Levine and Caves model can be used, with some modification, to treat the problem of gaseous diffusion in the alloy packs (ref. 9). We have taken the Al content of the Al-Ni particles in the depleted zone as that at the specimen surface. The amount of Al transferred from this zone is related to the difference between surface composition and pack composition. Details are given in Appendix A. Since the pack as well as the surface Al activity are variable, in the case of alloy packs, a series of K_g curves is obtained for each activator at a given temperature. By calculating both K_g and K_s as functions of surface composition, a predicted surface composition and rate constant

can be obtained, as with unalloyed Al packs.

Curves for AlF_3 activated alloy packs at 1093°C are shown in Fig. 23, theoretical and experimentally obtained surface compositions are compared in Fig. 8 and rate constants in Fig. 24. The observed surface Al concentrations are close to, but slightly (1-3 a/o) below the predicted concentrations, while both predicted and observed concentrations lie several atom percent below the expected equilibrium concentrations, i.e., the Al concentrations of the packs after 10 hr. pretreatment. These results modify the conclusions of Sivakumar and Seigle (ref. 7) who concluded on the basis of earlier experiments with AlF_3 activated alloy packs that for Al/Ni ratios below 50 a/o Al, the composition of the surface of the specimen was practically the same as that of the pack alloy and, therefore, that the rate of coating formation was controlled entirely by diffusion in the solid. The discrepancy between the present and earlier results is related to the use of unlined iron retorts in the earlier experiments. Evidently enough Al was exchanged between the pack and retort wall, when unlined retorts were used, to modify the pack Al concentration by a few a/o, sufficient to account for the difference observed. It is now concluded on the basis of both the theoretical calculations and present experimental results that in alloy packs even with a low Al:Ni ratio the surface Al concentration lies somewhat below the pack Al:Ni ratio and gas transport in the pack, as well as diffusion in the solid, must be considered in treating the kinetics of the process.

The fact that the details of gas transport in the pack must be taken into account in explaining the kinetics of the coating process in alloy packs is also suggested by the data of Figs. 2-5, in which it appears that the type of activator has an influence on the rate of aluminization at 1093°C. As shown most clearly in the results with the Raney alloy (Fig. 5), the fluoride activators usually produced the highest surface Al concentrations and coating rates followed by the chloride and then the iodide activators. This is the same order of effectiveness as observed with unalloyed Al packs and likewise attributable to the different rates of gas transport in the differently activated packs. Therefore the aluminization mechanism is essentially the same in alloy and unalloyed Al packs.

CONCLUDING REMARKS

This investigation of the pack aluminization of unalloyed Ni from packs of varying aluminum content, activated with various halide activators, leads to the conclusion that the kinetics of the pack aluminization process is controlled,under most circumstances, by a combination of gas diffusion in the pack and solid diffusion in the coating. If the rate of diffusion of gaseous halides in the pack is high, the surface of the coating tends to reach a high Al content whose value determines the type and rate of growth of intermetallic layers in the coating. The highest

gas diffusion rates and, therefore, the highest surface Al concentrations and highest coating rates are found with AlF_3 and NaF as activators, followed by NaCl and NaI in that order. The rate of gas diffusion in the pack, in turn, appears to be determined largely by the magnitude of the vapor pressures of the diffusing halides. Thus, the fluorides, in our experiments, were the most effective activators because the equilibrium vapor pressures of the fluorides in the pack were generally higher than the vapor pressures of chlorides or iodides.

The results of this work strongly confirm Levine and Cave's model for gas diffusion in the pack. By combining calculations of gas transport rates in the pack with calculations of solid diffusion rates the kinetics of the coating process can be completely defined. The theoretical equations have no adjustable parameters and their validity depends only upon the assumption of a time-invariant Al concentration at the surface of the coating, the presence of which is indicated by the experimental results. The theory is capable of making predictions about the influence of pack processing parameters, such as pack Al activity, type of activator, temperature, etc., in good agreement with experimental results for unalloyed Ni. In order to extend the theory to practical heat-resistant alloys, more information is needed concerning the thermodynamic properties and diffusivities of these alloys.

Appendix A

Calculation of Gas Diffusion Rate Constants

Pure Al packs:

According to the model of Levine and Caves (ref. 5) the parabolic rate constant for Al deposition is given by

$$K_g = \frac{2\rho\varepsilon M}{\tau RT} \sum \sigma_i D_i (P_i - P_i') \qquad (A1)$$

where D_i is the interdiffusion coefficient of species, i, P_i and P_i' are the partial pressures of the i^{th} Al-bearing species in the pack and at the specimen surface, resp., ρ is the pack Al density in gms/cm^3, ε and τ are correction factors for pack porosity and tortuosity, M is the gm-atomic weight of Al, T is temperature in degrees K, R is the gas constant and σ_i is a factor which allows for the fact that not all of the Al carried to the surface by gaseous species, i, enters the specimen. For NaX activators, i = 1, but for AlF_3 activated packs part of the Al transported by AlF(g) and AlF_2(g) contributes to the formation of AlF_3(s) at the surface of the specimen by the reactions,

$$3\ AlF(g) = AlF_3(s) + 2\ Al;\ \sigma_i = 2/3 \qquad (A2)$$

and

$$3\ AlF_2(g) = 2AlF_3(s) + Al;\ \sigma_i = 1/3 \qquad (A3)$$

Thus equation (A1) for AlF_3 activated packs is

$$K_g = \frac{2\rho\varepsilon M}{\tau RT}\left[\frac{2}{3} D_1 (P_{AlF} - P'_{AlF}) + \frac{1}{3} D_2 (P_{AlF_2} - P'_{AlF_2})\right] \qquad (A4)$$

To use the equations to calculate K_g, the partial pressures P_i and P_i' are needed. The method of calculating these depends on the type of activator used. For activators such as Na (F, Cl, I) and AlF_3, which are present in the pack as condensed phases at usual activator percentages and aluminizing temperatures, the partial pressures can be determined from the equilibrium constants of the reactions

$$NaX(l) + Al = AlX(g) + Na(g) \qquad (A5)$$

$$2\ NaX(l) + Al = AlX_2(g) + 2\ Na(g) \qquad (A6)$$

$$3\ NaX(l) + Al = AlX_3(g) + 3\ Na(g) \qquad (A7)$$

$$NaX(l) + 1/2\ H_2(g) = HX(g) + Na(g) \qquad (A8)$$

$$NaX(l) = NaX(g) \qquad (A9)$$

subject to the conditions,

$$P_{Na} = 3\,P_{AlX_3} + 2P_{AlX_2} + P_{AlX} + P_{HX} \qquad (A10)$$

$$\sum P_i = 1 \qquad (A11)$$

or, for the activator AlF_3,

$$AlF_3(g) + 2Al = 3AlF(g) \qquad (A12)$$

$$2AlF_3(g) + Al = 3\,AlF_2(g) \qquad (A13)$$

$$AlF_3(g) + 3/2\,H_2(g) = 3HF(g) + Al \qquad (A14)$$

$$AlF_3(s) = AlF_3(g) \qquad (A15)$$

subject to the condition $\sum P_i = 1$

To calculate partial pressures at the specimen surfaces, in the case of NaX activators in place of eq (A10) a mass balance condition is used:

$$D_{Na}\,(P_{Na}-P'_{Na}) = 3D_3\,(P_{AlX_3} - P'_{AlX_3}) + 2D_2\,(P_{AlX_2} - P_{AlX_2}) + D_1\,(P_{AlX} - P'_{AlX}) + D_{HX}\,(P_{HX} - P'_{HX}) \qquad (A16)$$

In principal a hydrogen balance equation should also be incorporated but this has been found unimportant since P_{H_2} is not far from 1 atm.

For activators such as NH_4Cl, with which no condensed phase is formed in the pack, it can be assumed, with semi-open retorts, that upon heating gases escape and the retort pressure remains at 1 atm. Upon heating, NH_4Cl dissociates according to the reactions

$$NH_4Cl(g) = NH_3(g) + HCl(g) \qquad (A17)$$

and

$$2NH_3(g) = N_2(g) + 3H_2(g) \qquad (A18)$$

Assuming that the atom ratio of H to Cl in the pack atmosphere remains the same as that in NH_4Cl, namely 4:1, the partial pressures in the pack can be obtained from the equations;

$$HCl(g) + Al = AlCl(g) + 1/2\ H_2(g) \qquad (A19)$$

$$2\ HCl(g) + Al = AlCl_2(g) + H_2(g) \qquad (A20)$$

$$3\ HCl(g) + Al = AlCl_3(g) + 3/2\ H_2(g) \qquad (A21)$$

subject to the conditions,

$$2\ P_{H_2} + P_{HCl} = 4\ (P_{AlCl} + 2\ P_{AlCl_2} + 3\ P_{AlCl_3} + P_{HCl}) \qquad (A22)$$

and

$$\sum P_i = 1 \qquad (A23)$$

For calculation of the partial pressures at the specimen surface, equ. (A22) and (A23) are replaced by the hydrogen and chlorine balances,

$$2\ D_{H_2}\ (P_{H_2} - P'_{H_2}) + D_{HCl}\ (P_{HCl} - P'_{HCl}) = 0 \qquad (A24)$$

$$D_{HCl}\ (P_{HCl} - P'_{HCl}) + D_{AlCl}\ (P_{AlCl} - P'_{AlCl}) + 2\ D_{AlCl_2}\ (P_{AlCl_2} - P_{AlCl_2}) + 3\ D_{AlCl_3}\ (P_{AlCl_3} - P'_{AlCl_3}) = 0 \qquad (A25)$$

The standard free energies of formation of the various compounds used in the calculations were taken from the JANAF tables (ref. 10). Vapour pressure data for $AlF_3(s)$ were obtained from Kubaschewski, et al. (Ref. 11). Values of the activities of Al in Ni-Al were calculated from the data of Steiner and Komarek (ref. 12). Calculated partial pressures in the pack and at the specimen surface are given in Tables V - IX.

For calculation of the gas diffusion rate constants, values of D_i were estimated from the Gilliland equation (ref. 13) assuming that interdiffusion occurred between the halide vapors and hydrogen as the major species. Estimated values of the interdiffusion coefficients are listed in Table X. Judging from the pack characteristics it was assumed that $\varepsilon = 0.70$ and $l = 4$. Values of K_g calculated from the above are given in Tables XI - XIV.

Alloy Packs:

Levine and Caves' model was extended to calculate rates of Al transport by gas diffusion in the alloy packs by assuming that Ni-Al particles in the depleted zone are of the same composition as the specimen surface. Fig. 25 shows schematic diagrams of the assumed Al-concentration profiles in pure Al and alloy packs. With this assumption the equation for K_g is equ. (Al) with the substitution

$$\rho = \rho_p - \rho_d \qquad \text{(A25)}$$

where ρ_p = gms/cm^3 Al in the undepleted pack and ρ_d = gms/cm^3 Al in the depleted zone. The partial pressures of gases in the undepleted pack, P_i are calculated as those in equilibrium with the pack Ni - Al alloy, whose aluminum activity is, of course, less than unity. The partial pressures, P'_i, are calculated as before.

Values of K_g were calculated for AlF_3 activated packs with Ni-Al alloy powders containing 43, 48, 52, 58 and 62 a/o Al. These represent the actual compositions of the powders following pretreatment of packs of nominal composition 45, 50, 55, 60 and 70 a/o Al, resp. Table XV lists the 1093°C calculated K_g values, and these are plotted in Fig. 23 as functions of surface composition.

APPENDIX B

Calculation of Solid Diffusion Rate Constants.

1) Inter-Diffusion Coefficients of Phases in the Ni-Al System.

Determination of the solid diffusion rate constant, K_S, requires a knowledge of the interdiffusion coefficients of the Ni_2Al_3 (γ), NiAl (δ), Ni_3Al (ε), and terminal solid solution (ζ) phases in the Ni-Al system. Average interdiffusion coefficients of phases in the system have been determined from layer growth measurements by Castleman and Seigle, Janssen and Rieck, Hickl and Heckel (ref. 14, 15, 16), and Janssen (ref. 17) has, in addition, determined the interdiffusion coefficient at a few specific compositions in the nickel-rich phases. It was felt, however, that more accurate data concerning the variation of the interdiffusion coefficient, D_δ with composition in the NiAl(δ) phase were required for the K_S calculations and measurements of this quantity were made by analysis of the concentration profiles of pack aluminized Ni and NiAl specimens.

The unalloyed Ni used was the same as that described previously, while the NiAl specimens were machined from arc-melted buttons containing 45.5, 47.2 and 49.4 a/o Al supplied by the NASA Lewis Research Center and United Aircraft Research Laboratories. Specimens were aluminized in AlF_3 activated alloy packs containing Al:Ni ratios varying from 55:45 to 70:30. Concentration profiles through the coating were determined by microprobe analysis of spots at 2 μm intervals along lines perpendicular to the surface of sectioned specimens. Typical concentration profiles are shown in Figs. 26 to 28.

Under the boundary conditions of constant surface concentration and diffusion into an infinitely extended medium, the diffusion coefficients may be extracted from the concentration profiles by application of the Boltzmann-Matano analysis, or Wagner's variation of this. For the aluminized Ni specimens with an extended range of concentrations in the coatings Wagner's equation (ref. 18) was used:

$$D = \frac{V}{2t\left(\frac{\partial N_{Al}}{\partial x}\right)}\left[(1-N_{Al})\int_{-\infty}^{x}\frac{N_{Al}}{V}\,dx + N_{Al}\int_{x}^{\infty}\frac{1-N_{Al}}{V}\,dx\right] \qquad (B1)$$

where N = atom fraction Al, V = molar volume, t = time and x is distance. For the aluminized NiAl specimens, the standard Boltzmann-Matano analysis was used:

$$D = \frac{1}{2t \frac{\partial N_{Al}}{\partial x}} \int_0^{N_{Al}} x \, d N_{Al} \qquad \text{(B2)}$$

in which χ is the distance measured from the Matano interface located under the assumption that no Ni is lost to the vapor phase (ref. 21).

The variation of D_δ with composition in the NiAl phase obtained by the above methods is shown in Figs. 29 and 30. It may be seen that D_δ varies over two orders of magnitude with composition. There is a pronounced minimum in the D vs. a/o Al curves which appears to fall slightly off the stoichiometric composition, on the low-Al side. Diffusion data from a variety of sources for the Ni-Al system are summarized in Fig. 31 which gives a good idea of the relative magnitudes of the D values in various phases of this system.

2) Calculation of K_s

Calculations of layer growth rates are usually made assuming that the interdiffusion coefficient, D_i, is a constant for each phase, i, (ref. 19,20). In the Ni Al(δ) phase the variation of D_δ with composition is so drastic, however, that a numerical method was devised to take this into account (ref. 21).

Fig. 32 represents the concentration profile of a coating whose surface composition lies in the δ phase field. In carrying out the calculations it is assumed that a constant average value of D may be used for the ε and ζ phases. The concentration profiles in these phases are, therefore, of the usual error function type:

$$N_\varepsilon = N_{\varepsilon\delta} - (N_{\varepsilon\delta} - N_{\varepsilon\zeta}) \frac{\{\mathrm{erf}(r_\varepsilon \alpha_{\delta\varepsilon}) - \mathrm{erf}(x/2\sqrt{D_\varepsilon t})\}}{\{\mathrm{erf}(r_\varepsilon \alpha_{\delta\varepsilon}) - \mathrm{erf}(r_\varepsilon \alpha_{\varepsilon\zeta})\}} \qquad \text{(B3)}$$

$$N_\zeta = N_{\zeta o} - (N_{\zeta o} - N_{\zeta\varepsilon}) \frac{\{1 - \mathrm{erf}(x/2\sqrt{D_\zeta t})\}}{\{1 - \mathrm{erf}(r_\zeta \alpha_{\varepsilon\zeta})\}} \qquad \text{(B4)}$$

where

$r_\varepsilon = \sqrt{D/D_\varepsilon}$; $r_\zeta = \sqrt{D/D_\zeta}$; $D = D_\delta$ $(N=N_{\delta\varepsilon})$; α_{ij} is a constant to be determined for each interface which governs the rate of interface movement according to the relationship, $x_{ij} = \partial\alpha_{ij}\sqrt{Dt}$. The D's in these equations are interdiffusion coefficients for the various phases, N is atom fraction Al and x is the distance from the Matano interface located using the condition that there is no transfer of Ni to the vapor phase (area A = Area B in Fig. 32).

Since D_δ varies strongly with composition the concentration profile in δ will not conform to an equation of type (B3) and is unlikely to obey any simple analytical expression. In this case it is expedient to seek a numerical solution of the diffusion equation for the δ phase and this is simplified if D_δ can be expressed as a function of composition. A reasonable fit of the diffusivity data is obtained by an expression of the type

$$D_\delta = D_o \exp(pN_\delta) \tag{B5}$$

for each branch of the diffusivity curve.

The diffusion equation in the δ phase

$$\frac{\partial N_\delta}{\partial t} = \frac{\partial}{\partial x}\left(D_\delta \frac{\partial N_\delta}{\partial x}\right) \tag{B6}$$

is then transformed to an ordinary differential equation

$$y\frac{d^2y}{dz^2} + \frac{2\alpha^2_{\delta\varepsilon}D}{D_o} z \frac{dy}{dz} = 0 \tag{B7}$$

by substitution of the new variables (ref. 22)

$$y = \exp(pN_\delta) \text{ and } z = x/2\alpha_{\delta\varepsilon}\sqrt{Dt} \quad (z = 1, \text{ at } x = x_{\delta\varepsilon}). \tag{B8}$$

To solve Eq. (B7, the following steps are carried out:

1) Using the error-function solutions (B3) and (B4) for the ε and ζ phases, Eq. (B9) may be written (ref. 21).

$$\alpha_{\varepsilon\zeta}(N_{\varepsilon\zeta} - N_{\zeta\varepsilon})\sqrt{\pi} = \frac{(N_{\varepsilon\xi} - N_{\varepsilon\zeta})\exp(-\gamma_\varepsilon^2\alpha_{\varepsilon\zeta}^2)}{\gamma_\varepsilon\{\mathrm{erf}(\gamma_\varepsilon\alpha_{\varepsilon\zeta}) - \mathrm{erf}(\gamma_\varepsilon\alpha_{\delta\varepsilon})\}}$$

$$= \frac{(N_{\zeta\varepsilon} - N_{\zeta o})\exp(-\gamma_\zeta^2\alpha_{\varepsilon\zeta}^2)}{\gamma_\zeta\{1 - \mathrm{erf}(\gamma_\zeta\alpha_{\varepsilon\zeta})\}} \qquad \text{(B9)}$$

with the two unknowns $\alpha_{\varepsilon\zeta}$ and $\alpha_{\delta\varepsilon}$. Choose a value of $\alpha_{\varepsilon\zeta}$ and calculate $\alpha_{\delta\varepsilon}$.

2) From mass balance conditions the concentration gradient in δ at the δ-ε interface may be written (ref. 21).

$$(dN_\delta/dz)_{z=1} = \frac{2\alpha_{\delta\varepsilon}(N_{\varepsilon\zeta} - N_{\varepsilon\delta})\exp(-\gamma_\varepsilon^2\alpha_{\delta\varepsilon}^2)}{\sqrt{\pi}\gamma_\varepsilon\{\mathrm{erf}(\gamma_\varepsilon\alpha_{\varepsilon\zeta}) - \mathrm{erf}(\gamma_\varepsilon\alpha_{\delta\varepsilon})\}}$$

$$- 2\alpha_{\delta\varepsilon}^2 (N_{\delta\varepsilon} - N_{\varepsilon\delta}). \qquad \text{(B10)}$$

3) Compute

$$(dy/dz)_{z=1} = p \exp(pN_{\delta\varepsilon})\cdot(dN_\delta/dz)_{z=1}. \qquad \text{(B11)}$$

4) The initial conditions for numerical solution of Eq.[B7] are the values of (dy/dz) and $y = y_1 = \exp(pN_{\delta\varepsilon})$ at $z = 1$. The differential equation is solved by the method of finite differences for decreasing values of z. Thus, at a small step Δz from the $\delta\varepsilon$ boundary, the value of y is given by:

$$y_2 = y_1 - \left(\frac{dy}{dz}\right)_{z=1} \Delta z .$$

Successive values of y can now be computed from the finite difference analog of the differential Eq.[B7]:

$$y_n \left\{ \frac{y_{n+1} - 2y_n + y_{n-1}}{\Delta z^2} \right\} + \frac{2\alpha^2_{\delta\varepsilon} D}{D_o} z_n \left\{ \frac{y_{n+1} - y_{n-1}}{2\Delta z} \right\} = 0. \quad \text{(B12)}$$

The solution is continued to the negative side of the z- axis, until the two areas A and B are equal (Fig. 32). This locates the specimen surface. The surface composition, $N_{\delta s}$, and α_s are obtained from the values of y and z at the surface. Steps [1] through [4] are then repeated with a new value of $\alpha_{\varepsilon\zeta}$. By this means a family of profiles is obtained corresponding to surface compositions over the entire homogeneity range of the δ phase. Concentration profiles for pack aluminization at 1100°C for 20 hours are shown in Fig. 33. It may be seen that the curves obtained from the numerical solution differ substantially from the usual error function type. By integrating the calculated composition profiles the Al intake and therefore K_s can be obtained for a given surface composition.

The numerical method is important only when NiAl (δ) is the surface layer of the coating. If the surface composition is such that Ni_2Al_3 is the first layer, then it is found that all the other layers develop relatively small thickness. In these cases a constant value of D_δ obtained by averaging the interdiffusion coefficient over the homogeneity range of the δ phase can be used with the standard equations for binary multiphase diffusion (ref. 19,20) in order to obtain the concentration profiles and K_s values.

References

1. Goward, G.W.; Boone, D.H. and Giggins, C.S.: Formation and Degradation Mechanisms of Aluminide Coatings on Nickel-Base Superalloys. Trans. ASM, vol. 60, 1967, pp228-241.

2. Goward, G.W. and Boone, D.H.: Mechanism of Formation of Diffusion Aluminide Coatings on Nickel-Base Superalloys. Oxidation of Metals, vol. 3, 1971, pp.475-495.

3. Walsh, P.N.: Chemical Vapor Deposition, Fourth International Conference; ed. by G.F. Wakefield and J.M. Blocker, Jr., The Electrochemical Society (New Jersey) 1970, pp. 147-168.

4. Brill-Edwards, H. and Epner, M: Effect of Materials Transfer Mechanisms on the Formation of Discontinuities in Pack Cementation Coatings on Superalloys. Electrochem. Tech., vol. 6, 1968, pp.299-307.

5. Levine, S.R. and Caves, R.M.: Thermodynamics and Kinetics of Pack Aluminide Coating on IN-100. J. Electrochem. Soc., vol.121, 1974, pp.1051-1064.

6. Colby, J.W.: Microprobe Analysis General Intensity Correction Program, Version 4. Bell Telephone Company, (Allentown, Pa.) 1969.

7. Sivakumar, R. and Seigle, L.L.: On the Kinetics of the Pack Aluminization Process. Met. Trans., vol. 7A, 1976, pp. 1073-1079.

8. Gupta, B.K.; Sarkhel, A.K. and Seigle, L.L.: On the Kinetics of Pack Aluminization. Thin Solid Films, vol. 39, 1976, pp.313-320.

9. Levine, S.R. and Seigle, L.L.: Kinetics of Pack Aluminization. Presented at the Annual Meeting of the American Ceramic Society, Washington, D.C., April 1975

10. JANAF Thermochemical Tables. Dow Chemical Co., (Midland, Mich.) 1972

11. Kubaschewski, O.; Evans, E.L.L. and Alcock, C.B.: Metallurgical Thermochemistry, 4th ed., Pergamon Press, N.Y., 1967

12. Steiner, A. and Komarek, K.L.: Thermodynamic Activities of Solid Nickel-Aluminum Alloys. Trans. Met. Soc. of AIME, vol. 230, 1964, pp.786-790.

13. Perry, R.H., and Chelton, C.H.: Chemical Engineers Handbook, McGraw-Hill, N.Y., 1973, pp.3-230.

14. Castleman, L.S. and Seigle, L.L.: Layer Growth During Interdiffusion In The Aluminum-Nickel Alloy System. Trans. Met. Soc. of AIME, vol. 212, 1958, pp. 589-596.

15. Janssen, M.M.P. and Rieck, G.D.: Reaction Diffusion and Kirkendall-Effect in the Nickel-Aluminum System. Trans. Met. Soc. of AIME, vol. 239, 1967, pp.1372-1385.

16. Hickl, A.J. and Heckl, R.W.: Kinetics of Phase Layer Growth During Aluminide Coating of Nickel. Met. Trans., vol. 6A, 1975, pp.431-440.

17. Janssen, M.M.P.: Diffusion in the Nickel-Rich Part of the Ni-Al System at 1000-1300°C; Ni_3Al Layer Growth, Diffusion Coefficients, and Interface Concentrations., Met. Trans., vol. 4, 1973, pp.1623-1633.

18. Wagner, C.: The Evaluation of Data Obtained with Diffusion Couples of Binary Single-Phase and Multiphase Systems., Acta Met., vol. 17, 1969.

19. Borisov, V.T.; Golikov, V.M. and Dubinin, G.N.: Determination of Diffusion Coefficients and Layer Thickness of the Phases in Reactive Diffusion. Diffusion Cladding of Metals, G.V. Samsonov, ed. Consultants Bureau, N.Y., 1967 pp.17-23.

20. Jost, W.: Diffusion in Solids, Liquids and Gases. Academic Press, N.Y., 1960.

21. Sarkhel, A.K. and Seigle, L.L.: Solution of Binary Multiphase Diffusion Problems Allowing for Variable Diffusivity, with Application to the Aluminization of Nickel. Met. Trans., vol. 7A, 1975, pp.899-902.

22. Wagner, C.: On the Solution of Diffusion Problems Involving Concentration-Dependent Diffusion Coefficients. Trans. AIME, vol.194, 1952, pp.91-96.

23. Swalin, R.A. and Martin, A.: Solute Diffusion in Nickel-Base Substitutional Solid Solutions. Trans. AIME, vol. 206, 1956, pp.567-572.

24. Sarkhel, A.K.: Ph.D. Thesis, State University of New York, Stony Brook, N.Y., 1977.

Table I. Pack composition after 10 hours pretreatment and 10 hours coating at 1093°C in alumina retorts (4 w/o AlF_3, metal:non-metal ratio - 50:50 w/o)

Nominal Pack Composition, a/o Al	Pack Composition after Pretreatment a/o Al	Pack Composition after Coating a/o Al	Surface Composition a/o Al
40	37.2	36.6	33.3
45	43.4	--	38.0
50	47.9	46.5	43.1
55	52.5	52.0	49.6
60	58.2	--	53.0
70	61.7 - Ni_2Al_3 75.0 - $NiAl_3$	61.5	58.4
Raney alloy	--	61.7	58.7

Table II. Comparison between the amount of aluminum removed from depleted zone and the actual weight gained by Ni specimen.

Experimental Conditions		Pack Data			Thickness of Depleted Zone, mm	Wt. of Al Removed from Depleted Zone, mg	Actual Wt. gain, mg
Temp. of Coating, °C	Time of Coating, hrs.	Activator	w/o Al in Pack	Pack Al Density, mg/cm^3			
1093	1/2	NaF	4	49.8	3.18	34.1	36.0
900	2	NaF	4	49.8	2.22	24.3	26.8
1000	1/2	NaF	4	49.8	1.28	16.0	19.3
1000	2	NaF	4	49.8	2.67	76.77	78.4
1000	5	NaF	10	131.3	0.44	27.0	30.0
1000	2	NaF	10	131.3	2.34	210.5	220.3
900	2	NaCl	4	39.65	0.47	6.4	6.6
900	10	NaCl	4	39.65	1.06	20.0	25.2
1000	2	NaCl	4	39.65	0.94	15.8	16.8
1000	5	NaCl	4	39.65	1.24	20.0	24.9
1000	10	NaCl	4	39.65	1.88	46.9	47.4
1000	20	NaCl	4	39.65	3.90	135.0	127.0
1000	2	NaCl	10	108.8	0.32	16.3	20.5
1000	5	NaCl	10	108.8	0.64	34.7	37.9
1000	10	NaCl	10	108.8	1.22	73.9	74.5
1000	20	NaCl	10	108.8	2.38	149.4	156.6

Table III. Comparison of theoretically predicted and observed surface composition (a/o Al), in pure Al packs (4 w/o activator, 40 mg/cm^3 pack Al density)

Coating Temp. °C	AlF_3		NaF		NaCl		NaI		NH_4Cl	
	Predicted	Observed	Predicted	Observed	Predicted	Observed	Predicted	Observed	Predicted	Observed
1093	Liquid >61.0	Liquid >61.0	Liquid >61.0	Liquid >61.0	55.4 (NiAl)	56.7 (NiAl)	55.30 (NiAl)	39.0 - 36.5	59.6	---
1000	62.0 (Ni_2Al_3)	59.8 (Ni_2Al_3)	61.1 (Ni_2Al_3)	59.5 (Ni_2Al_3)	55.2 (NiAl)	56.8 (NiAl)	54.9 (NiAl)	---	61.80	---
900	61.2 (Ni_2Al_3)	59.5-60.8 (Ni_2Al_3)	61.0 (Ni_2Al_3)	59.2 (Ni_2Al_3)	55.0 (NiAl)	55.3 (NiAl)	54.9 (NiAl)	---	63.2	---
800	60.7 (Ni_2Al_3)	59.3 (Ni_2Al_3)	60.5 (Ni_2Al_3)	58.5 (Ni_2Al_3)	54.8 (NiAl)	---	54.0 (NiAl)	---	Liquid Phase	---

Table IV. Comparison of theoretically predicted and observed K_{Al} values ($gm^2cm^{-4}hr^{-1}$) in pure Al packs (4 w/o activator, 40 mg/cm^3 pack Al density)

Coating Temp. °C	AlF_3		NaF		NaCl		NaI		NH_4Cl	
	Predicted	Observed	Predicted	Observed	Predicted	Observed	Predicted	Observed	Predicted	Observed
1093	---	*$3.75x10^{-3}$	---	$2.3x10^{-3}$*	$2.0x10^{-4}$	$6.17x10^{-6}$ - $5.2x10^{-4}$	$1.7x10^{-4}$	$1.46x10^{-5}$	$1.6x10^{-3}$	---
1000	$8.4x10^{-4}$	$8.6x10^{-4}$ - $8.1x^{10-4}$	$6.0x10^{-4}$	$9.5x10^{-4}$ - $8.0x10^{-4}$	$3.9x10^{-5}$	$1.70x10^{-4}$ - $1.02x10^{-4}$	$2.8x10^{-5}$	$3.72x10^{-6}$	$8.0x10^{-4}$	---
900	$1.7x10^{-4}$	$3.8x10^{-4}$ - $2.36x10^{-4}$	$1.6x10^{-4}$	$1.36x10^{-4}$ - $8.8x10^{-5}$	$8.8x10^{-6}$	$5.3x10^{-5}$ - $2.75x10^{-5}$	$8.9x10^{-6}$	---	$4.0x10^{-4}$	---
800	$3.0x10^{-5}$	$2.6x10^{-5}$	$2.4x10^{-5}$	$6.0x10^{-5}$ - $4.0x10^{-5}$	$1.6x10^{-6}$	---	$5.8x10^{-7}$	---	---	---

*Surface melting

Table V. Equilibrium partial pressure of gases in AlF_3 activated pure Al packs (atm)

Gases	Activity of Al a_{Al}	In the pack (P)			
		800°C	900°C	1000°C	1093°C
$P_{AlF}(g)$	1.0	1.16×10^{-3}	9.18×10^{-3}	5.18×10^{-2}	2.16×10^{-1}
$P_{AlF_2}(g)$	1.0	1.35×10^{-5}	2.27×10^{-3}	1.09×10^{-2}	1.71×10^{-2}
Vapour pressure of $AlF_3(c)$	1.0	7.05×10^{-5}	1.01×10^{-3}	9.51×10^{-3}	6.34×10^{-2}
		At the Coating Surface (P')			
$P_{AlF}(g)$	.5	7.35×10^{-4}	5.77×10^{-3}	3.26×10^{-2}	1.36×10^{-1}
	.1	2.51×10^{-4}	1.98×10^{-3}	1.11×10^{-2}	4.65×10^{-2}
	10^{-2}	5.40×10^{-5}	4.26×10^{-4}	2.4×10^{-3}	1.0×10^{-2}
	10^{-4}	2.51×10^{-6}	1.98×10^{-5}	1.11×10^{-4}	4.65×10^{-4}
$P_{AlF_2}(g)$	.5	1.07×10^{-5}	1.8×10^{-3}	8.66×10^{-3}	1.36×10^{-2}
	.1	6.27×10^{-6}	1.05×10^{-3}	5.06×10^{-3}	7.95×10^{-3}
	10^{-2}	2.91×10^{-6}	6.9×10^{-4}	2.35×10^{-3}	3.69×10^{-3}
	10^{-4}	6.27×10^{-7}	1.05×10^{-4}	5.06×10^{-4}	7.95×10^{-4}
Vapor Pressure of $AlF_3(c)$	.5	7.05×10^{-5}	1.01×10^{-3}	9.51×10^{-3}	6.34×10^{-2}
	.1				
	10^{-2}				
	10^{-4}				

Table VI. Equilibrium partial pressure of gases in NaF activated pure Al packs, (atm.)

Gases	Activity of Al, a_{Al}	In the pack (P)			
		800°C	900°C	1000°C	1093°C
$P_{AlF}(g)$	1.0	5.61×10^{-4}	6.45×10^{-3}	2.69×10^{-2}	7.14×10^{-2}
$P_{AlF_2}(g)$	1.0	5.38×10^{-5}	1.09×10^{-4}	6.31×10^{-4}	3.38×10^{-3}
$P_{AlF_3}(g)$	1.0	2.32×10^{-4}	3.50×10^{-4}	1.32×10^{-3}	2.41×10^{-3}
$P_{HF}(g)$	1.0	7.84×10^{-7}	2.53×10^{-6}	1.16×10^{-5}	4.5×10^{-5}
P_{Na}	1.0	2.04×10^{-3}	9.69×10^{-3}	3.21×10^{-2}	8.54×10^{-2}
		At the coating surface (P')			
$P_{AlF}(g)$	.5	1.26×10^{-4}	4.51×10^{-3}	1.90×10^{-2}	4.54×10^{-2}
	.1	3.33×10^{-5}	1.57×10^{-3}	7.80×10^{-3}	1.49×10^{-2}
	10^{-2}	3.9×10^{-6}	2.52×10^{-4}	1.85×10^{-3}	2.3×10^{-3}
	10^{-4}	4.29×10^{-8}	4.80×10^{-6}	7.50×10^{-5}	2.67×10^{-5}
$P_{AlF_2}(g)$	.5	3.15×10^{-5}	1.07×10^{-4}	6.01×10^{-4}	2.73×10^{-3}
	.1	1.10×10^{-5}	6.52×10^{-5}	5.37×10^{-4}	1.47×10^{-3}
	10^{-2}	1.51×10^{-6}	1.67×10^{-5}	2.98×10^{-4}	3.51×10^{-4}
	10^{-4}	1.83×10^{-8}	6.09×10^{-7}	1.66×10^{-5}	4.75×10^{-5}
$P_{AlF_3}(g)$	.5	3.55×10^{-4}	4.80×10^{-4}	1.86×10^{-3}	2.47×10^{-3}
	.1	1.64×10^{-4}	5.04×10^{-4}	3.28×10^{-3}	2.19×10^{-3}
	10^{-2}	2.65×10^{-5}	2.09×10^{-4}	4.28×10^{-3}	8.06×10^{-4}
	10^{-4}	3.53×10^{-7}	1.45×10^{-5}	2.87×10^{-3}	1.27×10^{-5}
$P_{Na}(g)$	.5	1.89×10^{-3}	6.92×10^{-3}	2.27×10^{-2}	6.72×10^{-2}
	.1	1.43×10^{-3}	3.98×10^{-3}	1.1×10^{-2}	4.09×10^{-2}
	10^{-2}	1.22×10^{-3}	2.48×10^{-3}	4.67×10^{-3}	2.65×10^{-2}
	10^{-4}	1.11×10^{-3}	1.30×10^{-3}	1.15×10^{-3}	2.28×10^{-2}

Table VII. Equilibrium partial pressure of gases in NaCl activated pure Al packs, (atm.)

Gases	Activity of Al, a_{Al}	In The Pack (P)			
		800°C	900°C	1000°C	1093°C
$P_{AlCl}(g)$	1.0	4.19×10^{-5}	2.57×10^{-4}	1.17×10^{-3}	4.19×10^{-3}
$P_{AlCl_2}(g)$	1.0	8.28×10^{-6}	2.33×10^{-5}	1.08×10^{-4}	8.63×10^{-4}
$P_{AlCl_3}(g)$	1.0	6.19×10^{-8}	1.12×10^{-7}	4.89×10^{-7}	3.44×10^{-6}
$P_{HCl}(g)$	1.0	8.82×10^{-7}	2.92×10^{-6}	1.11×10^{-5}	3.52×10^{-5}
$P_{Na}(g)$	1.0	5.96×10^{-5}	3.08×10^{-4}	1.41×10^{-3}	5.95×10^{-3}
		At The Coating Surface (P')			
P_{AlCl} (g)	.5	2.63×10^{-5}	1.74×10^{-4}	7.93×10^{-4}	2.64×10^{-3}
	.1	7.79×10^{-6}	6.49×10^{-5}	3.0×10^{-4}	7.88×10^{-4}
	10^{-2}	9.8×10^{-7}	1.37×10^{-5}	6.15×10^{-5}	1.02×10^{-4}
	10^{-4}	1.02×10^{-8}	2.02×10^{-7}	9.7×10^{-7}	1.06×10^{-6}
$P_{AlCl_2}(g)$	.5	6.53×10^{-6}	2.14×10^{-5}	9.9×10^{-5}	6.83×10^{-4}
	.1	2.85×10^{-6}	1.48×10^{-5}	7.11×10^{-5}	3.06×10^{-4}
	10^{-2}	4.52×10^{-7}	6.63×10^{-6}	2.98×10^{-5}	5.10×10^{-6}
	10^{-4}	4.90×10^{-9}	1.44×10^{-7}	7.4×10^{-7}	5.49×10^{-8}
$P_{AlCl_3}(g)$	.5	6.12×10^{-8}	1.39×10^{-7}	6.1×10^{-7}	3.42×10^{-6}
	.1	3.97×10^{-8}	1.31×10^{-7}	8.3×10^{-7}	2.28×10^{-6}
	10^{-2}	7.89×10^{-9}	1.30×10^{-7}	7.13×10^{-7}	4.94×10^{-7}
	10^{-4}	8.9×10^{-11}	6.2×10^{-8}	2.79×10^{-8}	5.54×10^{-9}
$P_{Na}(g)$	.5	4.75×10^{-5}	2.27×10^{-4}	1.04×10^{-3}	4.73×10^{-3}
	.1	3.21×10^{-5}	1.22×10^{-4}	5.49×10^{-4}	3.17×10^{-3}
	10^{-2}	2.55×10^{-5}	5.77×10^{-5}	2.68×10^{-4}	2.45×10^{-3}
	10^{-4}	2.45×10^{-5}	3.91×10^{-5}	1.70×10^{-4}	2.36×10^{-3}

Table VIII. Equilibrium partial pressure of gases in NaI activated pure Al packs, (atm.)

Gases	Activity of Al, a_{Al}	In the Pack (P)			
		800°C	900°C	1000°C	1093°C
$P_{AlI}(g)$	1.0	2.02×10^{-5}	2.97×10^{-4}	1.33×10^{-3}	4.95×10^{-3}
$P_{AlI_3}(g)$	1.0	3.56×10^{-9}	4.11×10^{-10}	2.36×10^{-9}	1.22×10^{-8}
$P_{HI}(g)$	1.0	1.19×10^{-6}	1.47×10^{-6}	5.79×10^{-6}	1.91×10^{-5}
$P_{Na}(g)$	1.0	2.13×10^{-4}	2.98×10^{-4}	1.33×10^{-3}	4.98×10^{-3}
		At the Coating Surface			
$P_{AlI}(g)$	.5	1.24×10^{-5}	2.0×10^{-4}	1.06×10^{-3}	3.06×10^{-3}
	.1	3.28×10^{-6}	7.42×10^{-5}	5.7×10^{-4}	8.51×10^{-4}
	10^{-2}	3.61×10^{-7}	1.26×10^{-5}	6.58×10^{-5}	9.84×10^{-5}
	10^{-4}	3.74×10^{-9}	1.45×10^{-7}	6.7×10^{-7}	1.0×10^{-6}
$P_{AlI_3}(g)$	.5	3.32×10^{-9}	5.11×10^{-10}	3.5×10^{-8}	1.16×10^{-8}
	.1	1.53×10^{-9}	6.47×10^{-10}	1.86×10^{-8}	6.24×10^{-9}
	10^{-2}	2.04×10^{-10}	3.17×10^{-10}	2.85×10^{-9}	9.64×10^{-10}
	10^{-4}	2.26×10^{-12}	4.48×10^{-12}	3.0×10^{-11}	1.02×10^{-11}
$P_{Na}(g)$	.5	1.73×10^{-5}	2.2×10^{-4}	4.29×10^{-4}	4.02×10^{-3}
	.1	1.31×10^{-5}	1.19×10^{-4}	3.10×10^{-4}	2.89×10^{-3}
	10^{-2}	1.19×10^{-5}	7.0×10^{-5}	2.69×10^{-4}	2.5×10^{-3}
	10^{-4}	1.15×10^{-5}	6.08×10^{-5}	2.64×10^{-4}	2.45×10^{-3}

Table IX. Equilibrium partial pressure of gases in NH_4Cl activated pure Al packs (atm.)

Gases	Activity of Al, a_{Al}	In the Pack (P)			
		800°C	900°C	1000°C	1093°C
$P_{AlCl}(g)$	1.0	1.13×10^{-2}	2.86×10^{-2}	4.89×10^{-2}	7.91×10^{-2}
$P_{AlCl_2}(g)$	1.0	9.25×10^{-2}	1.23×10^{-1}	1.37×10^{-1}	1.36×10^{-1}
$P_{AlCl_3}(g)$	1.0	7.17×10^{-2}	4.27×10^{-3}	2.37×10^{-2}	1.12×10^{-2}
$P_{HCl}(g)$	1.0	4.96×10^{-4}	5.60×10^{-4}	5.83×10^{-4}	5.75×10^{-4}
$P_{H_2}(g)$	1.0	0.8239	0.8053	0.7896	0.7725
		At the Coating Surface (P')			
P_{AlCl}	.5	7.49×10^{-3}	1.95×10^{-2}	3.42×10^{-2}	5.71×10^{-2}
	.1	2.77×10^{-3}	7.59×10^{-3}	1.41×10^{-2}	2.5×10^{-2}
	10^{-2}	6.33×10^{-3}	1.82×10^{-3}	3.57×10^{-3}	6.79×10^{-3}
	10^{-4}	3.04×10^{-5}	9.02×10^{-5}	1.85×10^{-4}	3.74×10^{-4}
$P_{AlCl_2}(g)$	.5	8.07×10^{-2}	1.14×10^{-1}	1.34×10^{-1}	1.42×10^{-1}
	.1	5.50×10^{-2}	8.65×10^{-2}	1.41×10^{-1}	1.37×10^{-1}
	10^{-2}	2.88×10^{-2}	4.96×10^{-2}	7.30×10^{-2}	1.00×10^{-1}
	10^{-4}	6.63×10^{-3}	1.22×10^{-2}	1.95×10^{-2}	3.06×10^{-2}
$P_{AlCl_3}(g)$	.5	8.25×10^{-2}	5.38×10^{-2}	3.26×10^{-2}	1.68×10^{-2}
	.1	1.04×10^{-1}	7.99×10^{-2}	5.71×10^{-2}	3.55×10^{-2}
	10^{-2}	1.24×10^{-1}	1.10×10^{-1}	9.24×10^{-2}	7.07×10^{-2}
	10^{-4}	1.37×10^{-1}	1.34×10^{-1}	1.28×10^{-1}	1.18×10^{-1}
P_{HCl}	.5	6.55×10^{-4}	7.62×10^{-4}	8.17×10^{-4}	8.30×10^{-4}
	.1	1.21×10^{-3}	1.48×10^{-3}	1.68×10^{-3}	1.82×10^{-3}
	10^{-2}	2.76×10^{-3}	3.56×10^{-3}	4.26×10^{-3}	4.93×10^{-3}
	10^{-4}	1.32×10^{-2}	1.76×10^{-2}	2.19×10^{-2}	2.70×10^{-2}
P_{H_2}	.5	0.8238	0.8053	0.7895	0.7724
	.1	0.8236	0.8050	0.7893	0.7721
	10^{-2}	0.8217	0.8044	0.7885	0.7711
	10^{-4}	0.8199	0.7999	0.7829	0.7689

Table X. Calculated interdiffusion coefficient (D_i) for different gaseous systems.

Gaseous Species	D_i cm^2/sec			
	1093°C	1000°C	900°C	800°C
H_2-AlF	5.77	5.19	4.59	4.02
H_2-AlF_2	5.07	4.56	4.03	3.53
H_2-AlF_3	4.59	4.13	3.65	3.19
H_2-HF	5.52	4.96	4.39	3.84
H_2-AlCl	4.83	4.35	3.84	3.36
H_2-$AlCl_2$	3.96	3.56	3.15	2.76
H_2-$AlCl_3$	3.45	3.10	2.75	2.40
H_2-HCl	4.16	3.74	3.31	2.89
H_2-AlI	4.14	3.73	3.29	2.88
H_2-AlI_3	2.80	2.52	2.23	1.95
H_2-HI	3.82	3.44	3.04	2.66

Table XI. Theoretical aluminum deposition rate constant for gaseous and solid diffusion in pure Al packs at 800°C (4 w/o activator, 40 mg/cm^3 pack Al density)

Surface Comp. a/o Al	Gaseous Diffusion Rate Constant, K_{gas}, $gm^2cm^{-4}hr^{-1}$					K_{solid}, $gm^2cm^{-4}hr^{-1}$
	AlF_3	NaF	NaCl	NaI	NH_4Cl	
45	$5.50x10^{-5}$	$3.75x10^{-5}$	$1.95x10^{-6}$	$6.99x10^{-7}$	$1.0x10^{-3}$	$1.6\ x10^{-7}$
50	$5.05x10^{-5}$	$3.47x10^{-5}$	$1.89x10^{-6}$	$6.80x10^{-7}$	$8.6x10^{-4}$	$1.65x10^{-7}$
55	$4.00x10^{-5}$	$2.78x10^{-5}$	$1.37x10^{-6}$	$5.42x10^{-7}$	$6.8x10^{-4}$	$1.8\ x10^{-6}$
60	$3.38x10^{-5}$	$2.45x10^{-5}$	$1.13x10^{-6}$	$4.60x10^{-7}$	$4.9x10^{-4}$	$1.75x10^{-5}$
61	$2.85x10^{-5}$	$2.15x10^{-5}$	$9.30x10^{-7}$	$3.91x10^{-7}$	$4.2x10^{-4}$	$3.7\ x10^{-5}$

Table XII. Theoretical Al deposition rate constant for gaseous and solid diffusion in pure Al packs at 900°C (4 w/o activator, 40 mg/cm^3 pack Al density)

Surface Comp. a/o Al	Gaseous Diffusion Rate Constant, K_{gas}, $gm^2cm^{-4}hr^{-1}$					K_{solid}, $gm^2cm^{-4}hr^{-1}$
	AlF_3	NaF	NaCl	NaI	NH_4Cl	
45	3.3×10^{-4}	3.1×10^{-4}	1.1×10^{-5}	1.0×10^{-5}	2.15×10^{-3}	5.1×10^{-7}
50	3.1×10^{-4}	3.0×10^{-4}	1.03×10^{-5}	9.5×10^{-6}	1.55×10^{-3}	5.7×10^{-7}
55	2.8×10^{-4}	2.65×10^{-4}	8.8×10^{-5}	8.2×10^{-6}	1.12×10^{-3}	8.5×10^{-6}
60	2.2×10^{-4}	2.1×10^{-4}	7.0×10^{-6}	6.8×10^{-6}	8.2×10^{-4}	5.7×10^{-5}
61	1.85×10^{-4}	1.7×10^{-4}	5.8×10^{-6}	5.5×10^{-6}	6.8×10^{-4}	1.25×10^{-4}

Table XIII. Theoretical Al deposition rate constant for diffusion in gas and solid phases with different activators at 1000°C (4 w/o activator, 40 mg/cm^3 pack Al density)

Surface Comp. a/o Al	Gaseous Diffusion Rate Constant, K_{gas}, $gm^2cm^{-4}hr^{-1}$					K_{solid}, $gm^2cm^{-4}hr^{-1}$
	AlF_3	NaF	NaCl	NaI	NH_4Cl	
45	2.1×10^{-3}	1.42×10^{-3}	5.95×10^{-5}	5.4×10^{-5}	3.2×10^{-3}	2.5×10^{-6}
50	1.95×10^{-3}	1.35×10^{-3}	5.4×10^{-5}	4.3×10^{-5}	2.3×10^{-3}	2.65×10^{-6}
55	1.45×10^{-3}	9.0×10^{-4}	4.0×10^{-5}	2.7×10^{-5}	1.75×10^{-3}	3.2×10^{-5}
60	1.23×10^{-3}	7.4×10^{-4}	3.3×10^{-5}	2.25×10^{-5}	1.25×10^{-3}	3.2×10^{-5}
61	1.05×10^{-3}	6.1×10^{-4}	2.75×10^{-5}	1.9×10^{-5}	9.8×10^{-4}	5.8×10^{-5}

Table XIV. Theoretical Al deposition rate constants for diffusion in gas and solid phases with different activators at 1093°C (4 w/o activator, 40 mg/cm^3 pack Al density)

Surface Comp. a/o Al	Gaseous Diffusion Rate Constant, K_{gas}, $gm^2cm^{-4}hr^{-1}$					K_{solid}, $gm^2cm^{-4}hr^{-1}$
	AlF_3	NaF	NaCl	NaI	NH_4Cl	
45	$1.12x10^{-2}$	$5.1\ x10^{-3}$	$2.81x10^{-4}$	$2.42x10^{-4}$	$4.6\ x10^{-3}$	$1.5\ x10^{-5}$
50	$1.04x10^{-2}$	$4.7\ x10^{-3}$	$2.65x10^{-4}$	$2.33x10^{-4}$	$2.8\ x10^{-3}$	$1.55x10^{-5}$
55	$7.95x10^{-3}$	$3.65x10^{-3}$	$2.0\ x10^{-4}$	$1.73x10^{-4}$	$1.8\ x10^{-3}$	$1.15x10^{-4}$
60	$6.8\ x10^{-3}$	$3.05x10^{-3}$	$1.68x10^{-4}$	$1.51x10^{-4}$	$1.55x10^{-3}$	$1.75x10^{-3}$
61	$5.6\ x10^{-3}$	$2.57x10^{-3}$	$1.4\ x10^{-4}$	$1.25x10^{-4}$	$1.15x10^{-3}$	$2.4\ x10^{-3}$

Table XV. Theoretical aluminum deposition rate constant for gaseous and solid diffusion in AlF_3 activated alloy packs. (4 w/o activator, metal: non-metal ratio, 50:50 w/o, 1093°C)

Pack† Comp. a/o Al	Nominal Pack Comp. a/o	Surface Comp. a/o Al	K_{gas}, $gm^2\ cm^{-4}\ hr^{-1}$	K_{solid}, $gm^2\ cm^{-4}\ hr^{-1}$
43	45	35	2.1×10^{-5}	---
		37	1.5×10^{-5}	6.1×10^{-6}
		39	8.6×10^{-6}	1.0×10^{-5}
		40	5.6×10^{-6}	1.14×10^{-5}
48	50	40	1.5×10^{-4}	1.14×10^{-5}
		42	1.0×10^{-4}	1.33×10^{-5}
		43	8.6×10^{-5}	1.4×10^{-5}
		45	4.4×10^{-5}	1.5×10^{-5}
		47	7.8×10^{-7}	1.52×10^{-5}
52	55	43	2.0×10^{-3}	1.4×10^{-5}
		45	1.6×10^{-3}	1.5×10^{-5}
		47	1.1×10^{-3}	1.52×10^{-5}
		49	6.1×10^{-4}	1.54×10^{-5}
		50	2.8×10^{-4}	1.57×10^{-5}
		51	3.9×10^{-5}	1.62×10^{-5}
58	60	45	5.6×10^{-3}	1.5×10^{-5}
		47	4.5×10^{-3}	1.52×10^{-5}
		50	2.65×10^{-3}	1.57×10^{-5}
		53	7.3×10^{-4}	2.35×10^{-5}
		55	2.0×10^{-4}	1.15×10^{-4}
		56	4.3×10^{-4}	3.65×10^{-4}
62	70	50	8.6×10^{-3}	1.57×10^{-5}
		53	5.2×10^{-3}	2.35×10^{-5}
		55	3.6×10^{-3}	1.15×10^{-4}
		56	2.9×10^{-3}	3.65×10^{-4}
		60	8.1×10^{-4}	1.7×10^{-3}
		61	1.95×10^{-4}	2.4×10^{-3}

†Pack composition after pretreatment at 1093°C

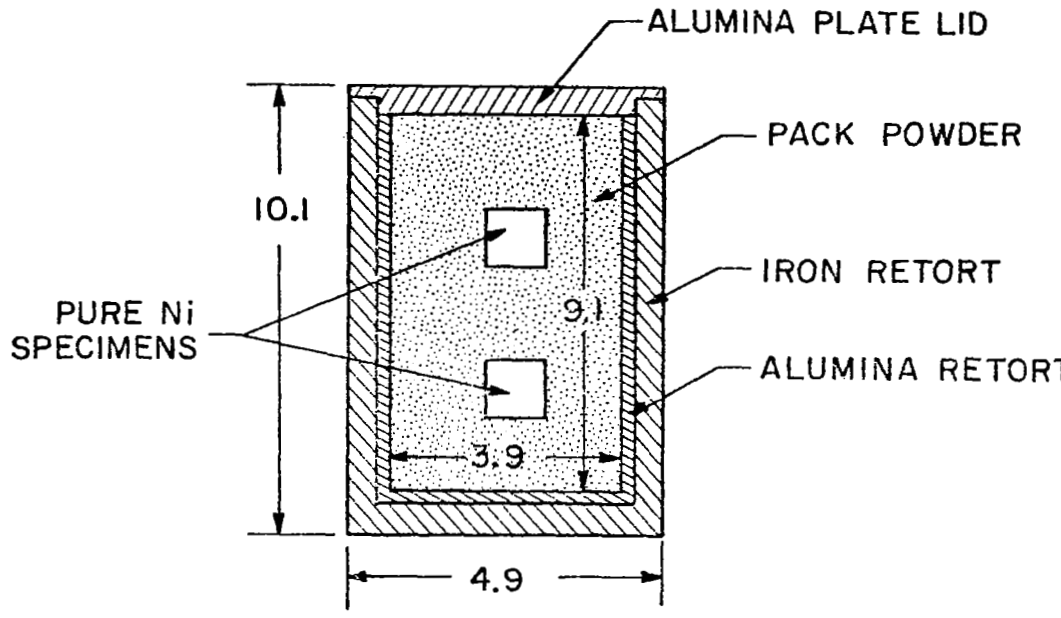

ALUMINA RETORT ASSEMBLY

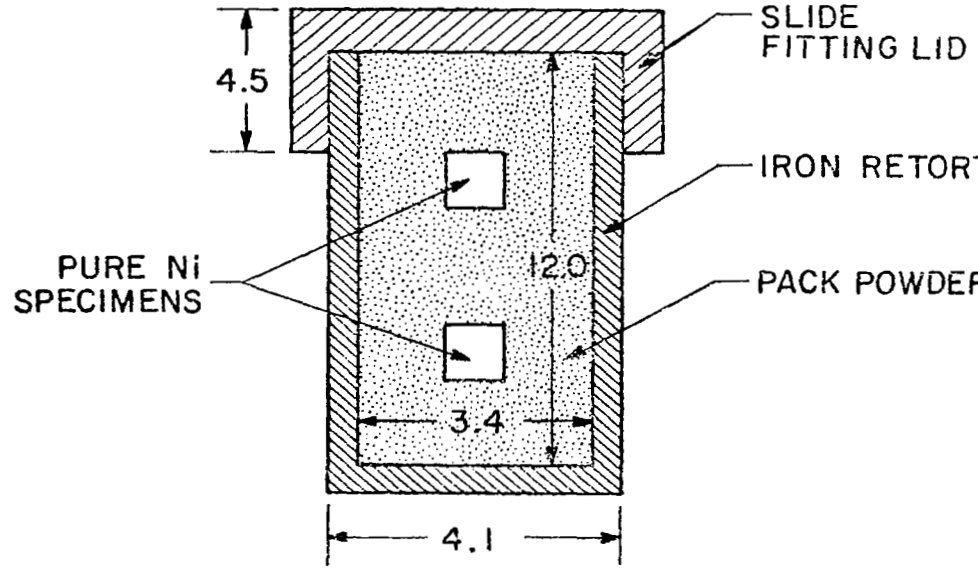

IRON RETORT ASSEMBLY

(Dimensions in cms)

Fig. 1 - Aluminizing Retort Assemblies

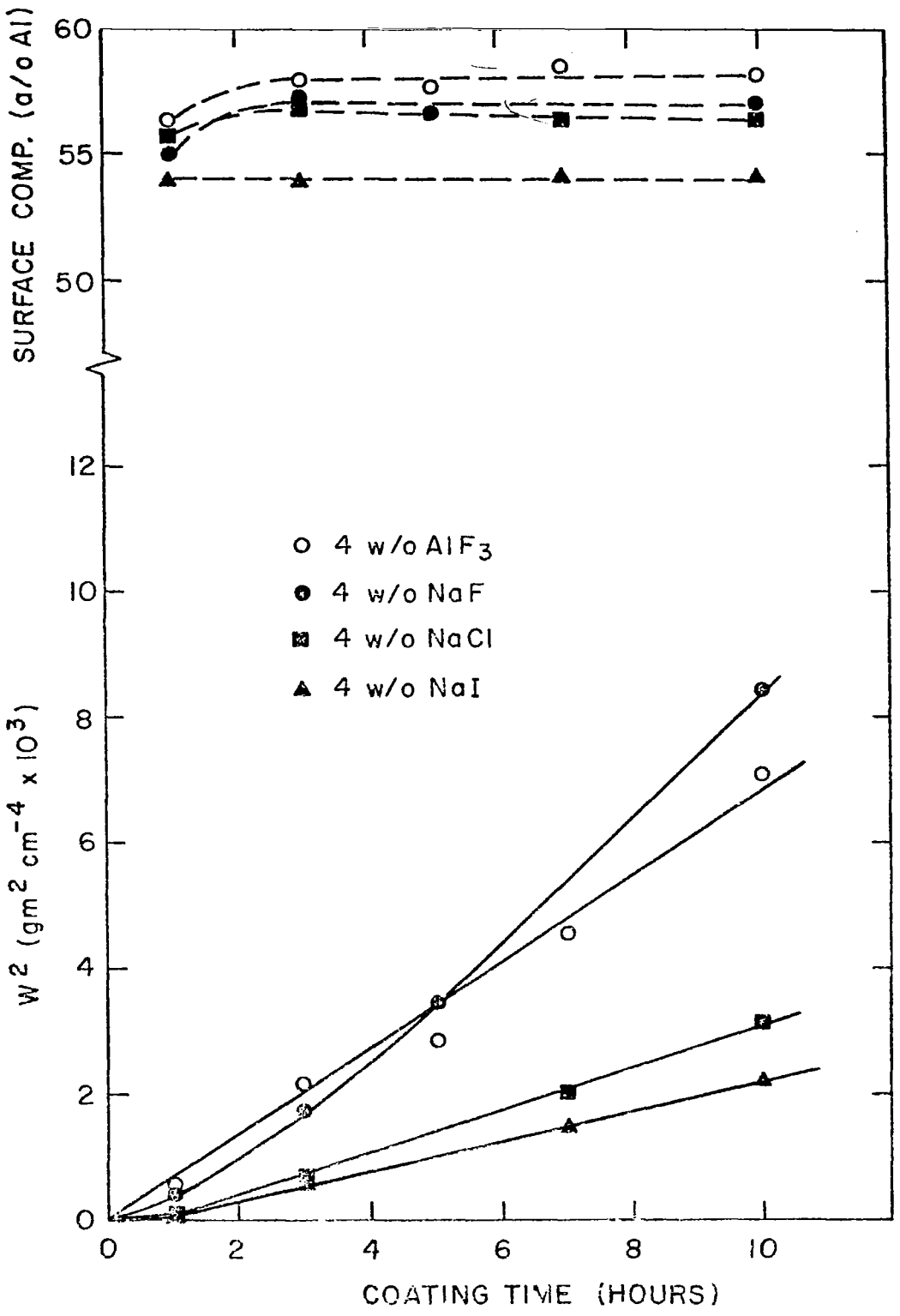

Fig. 2 - Variation of W^2 and Surface Composition with Time in 70 Al/30 Ni Packs at 1093°C.

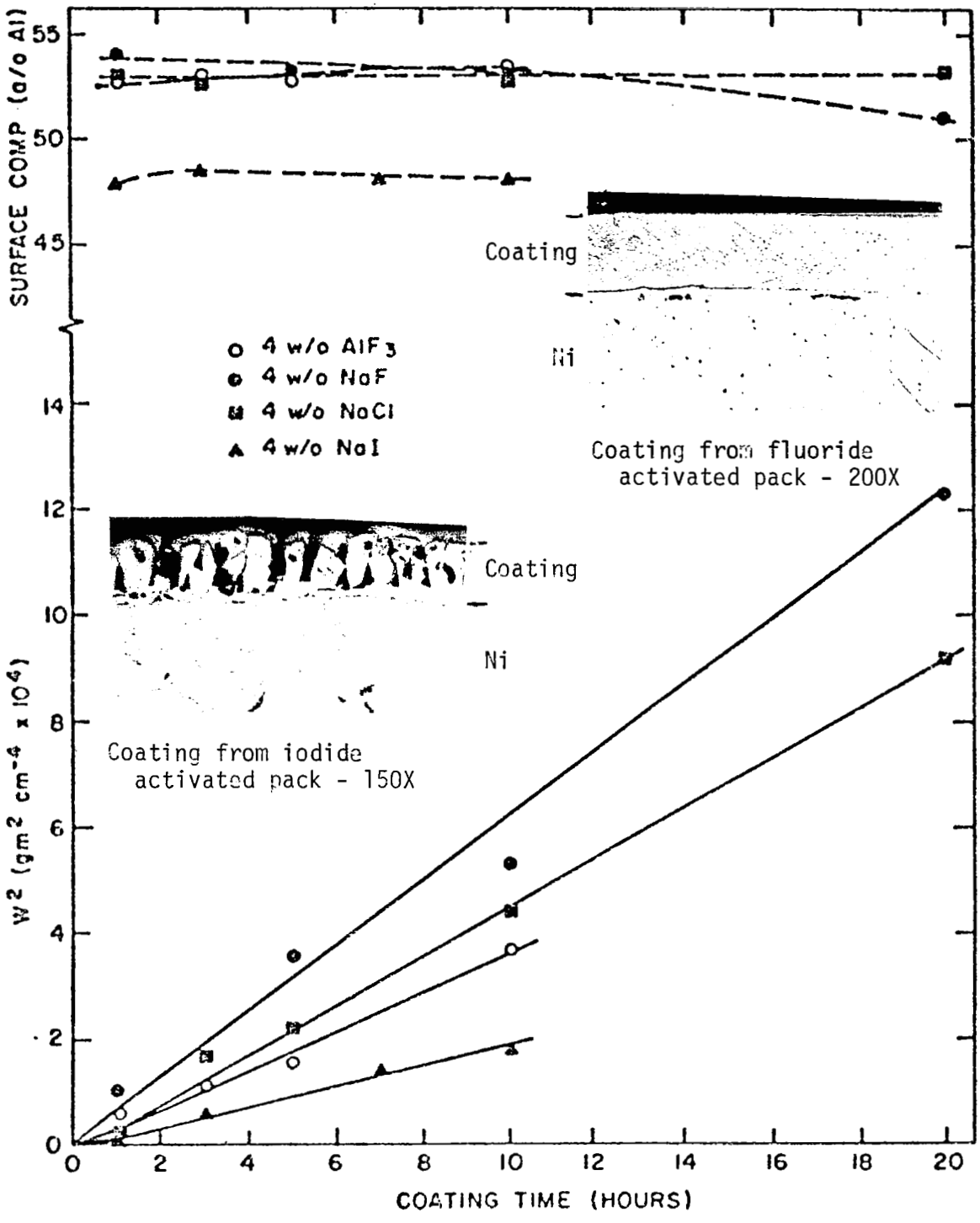

Fig. 3 - Variation of W^2 and Surface Composition with Time in 60 Al/40 Ni Packs at 1093°C.

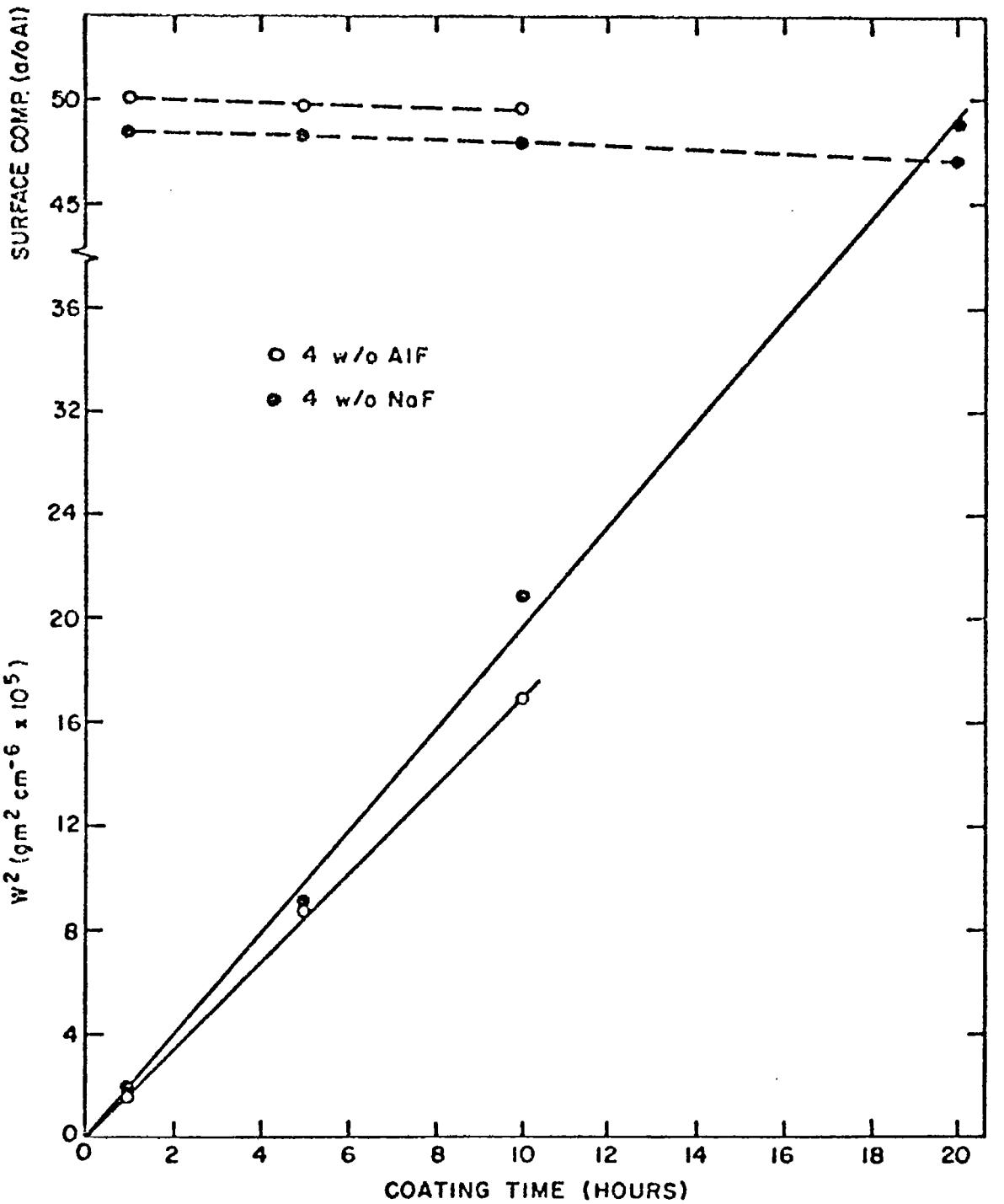

Fig. 4 - Variation of W^2 and Surface Composition with Time in 55 Al/45 Ni Packs at 1093°C.

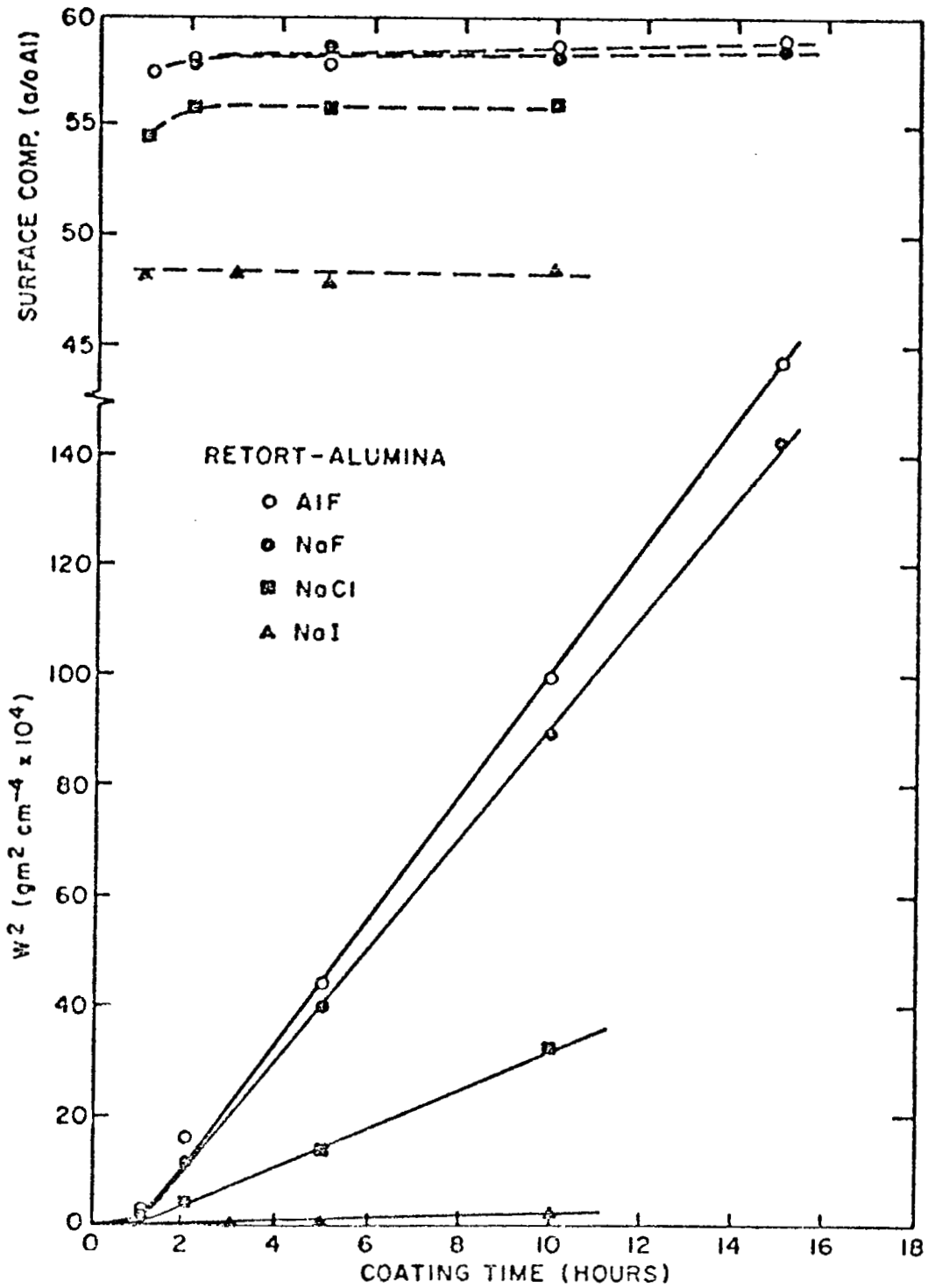

Fig. 5 - Variation of W^2 and Surface Composition with Time in Raney Alloy (69 Al/31 Ni) Packs at 1093°C.

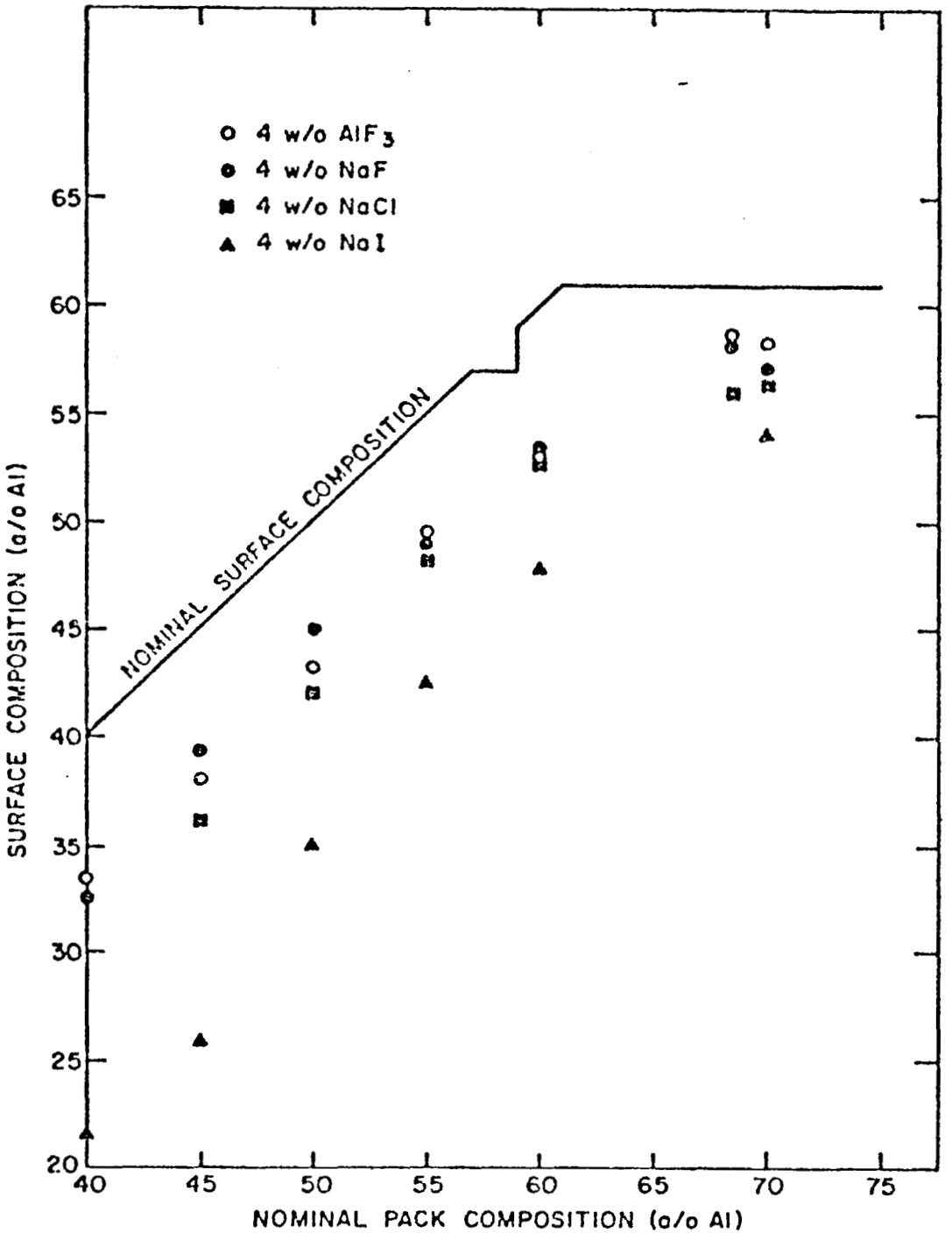

Fig. 6 - Relationship Between Surface and Pack Composition After Aluminization for 10 hrs. at 1093°C.

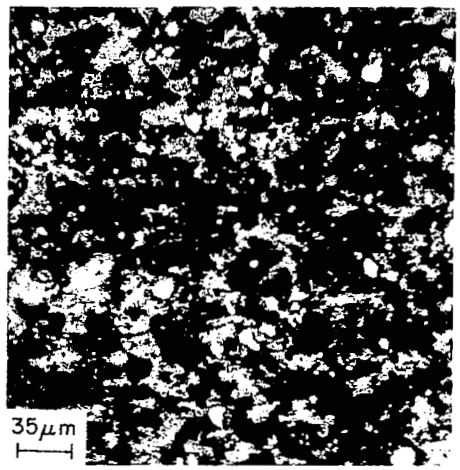

50 Al/50 Ni

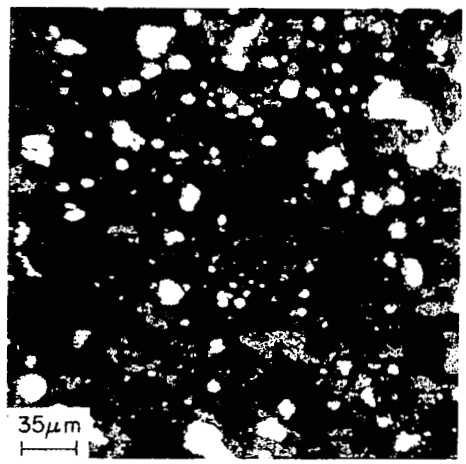

60 Al/40 Ni

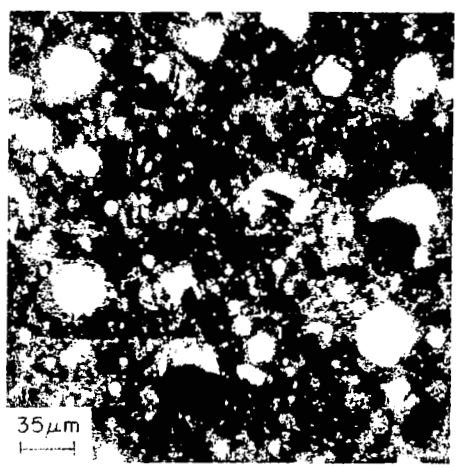

70 Al/30 Ni

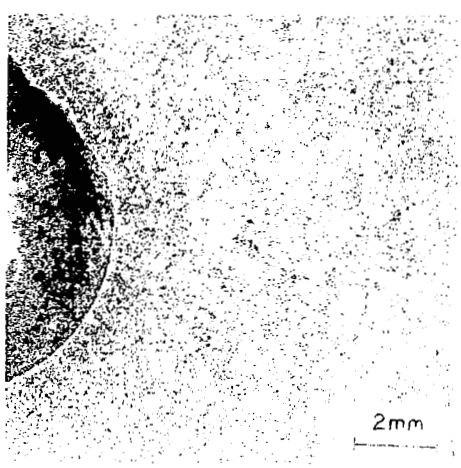

50 Al/50 Ni

Fig. 7 - Alloy Distribution in Ni/Al Alloy Packs after 10 hrs. at 1093°C.

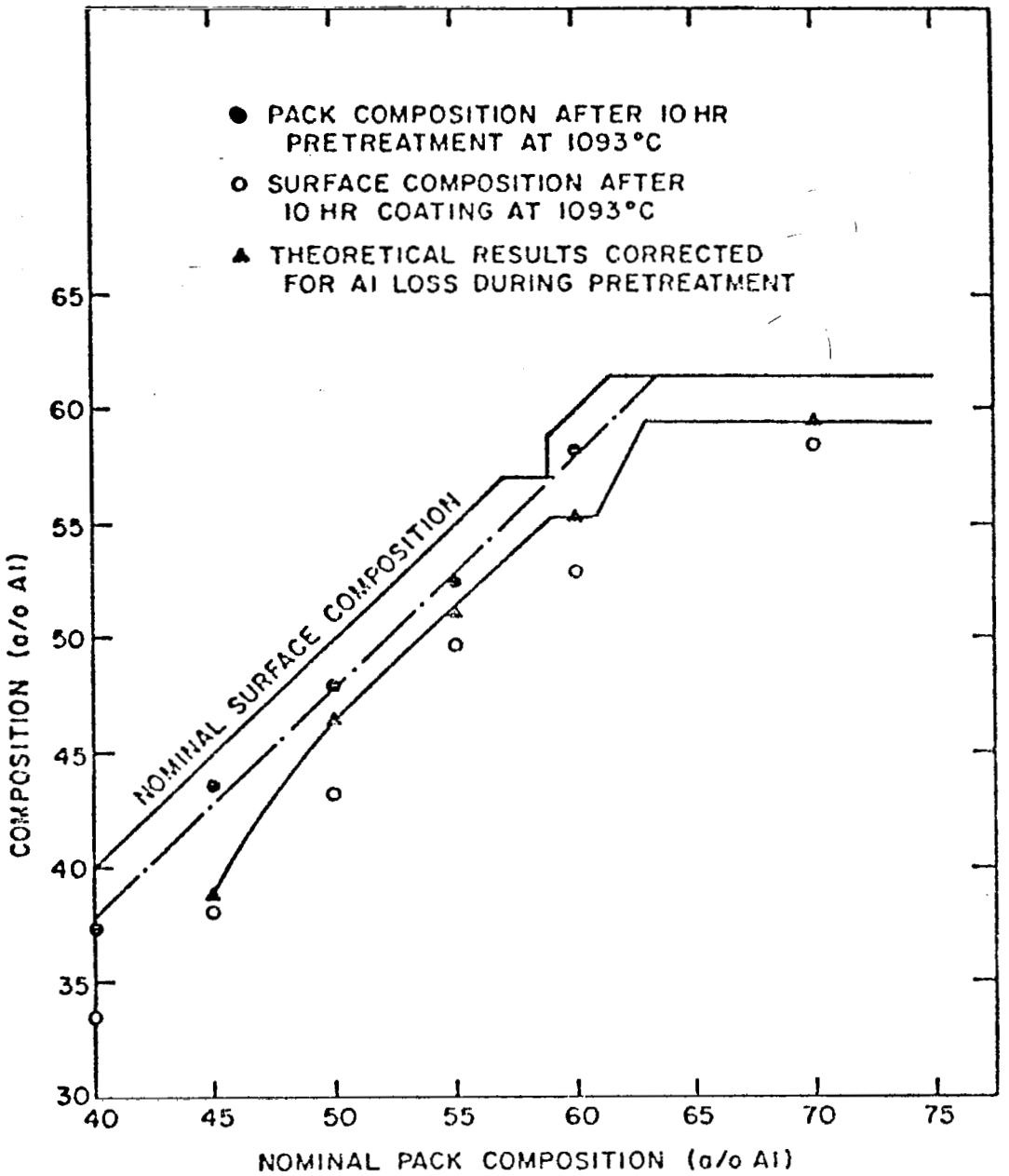

Fig. 8 - Comparison of Theoretical and Observed Surface Compositions after Aluminization for 10 hrs. at 1093°C in 4 w/o AlF_3 Activated Packs.

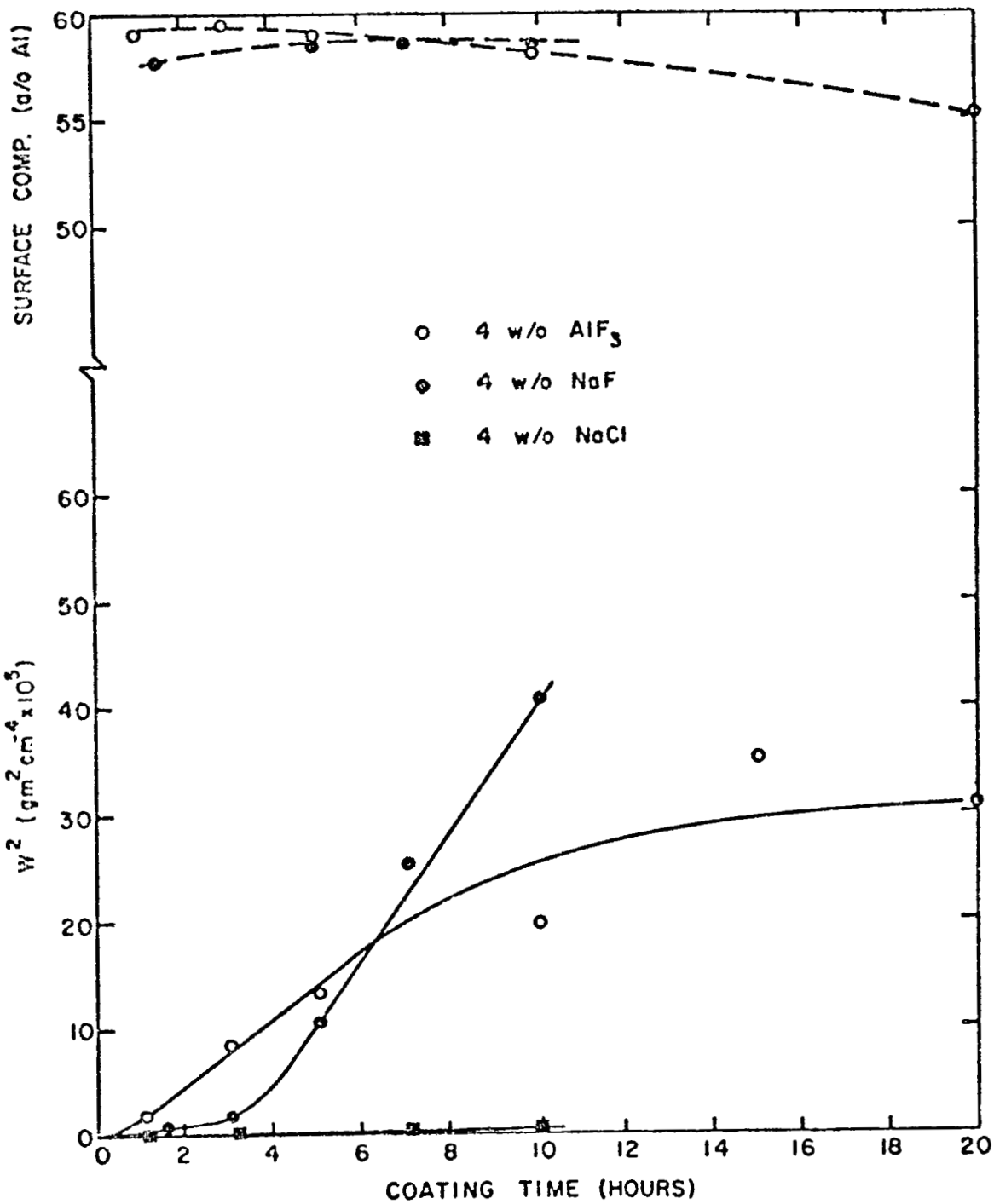

Fig. 9 - Variation of W^2 and Surface Composition With Time in 4 w/o Al Packs at 800°C.

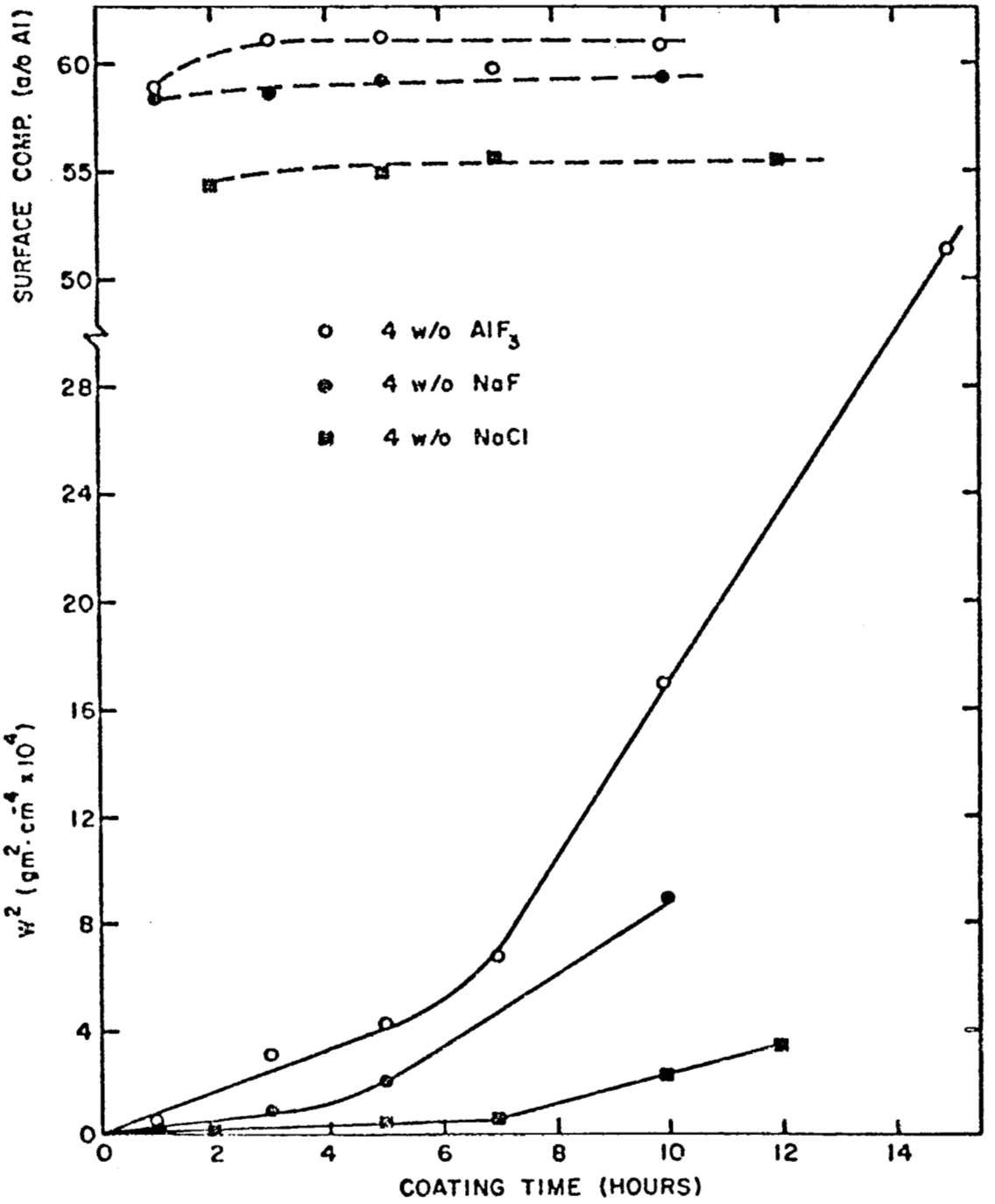

Fig. 10 - Variation of W^2 and Surface Composition With Time in 4 w/o Al Packs at 900°C.

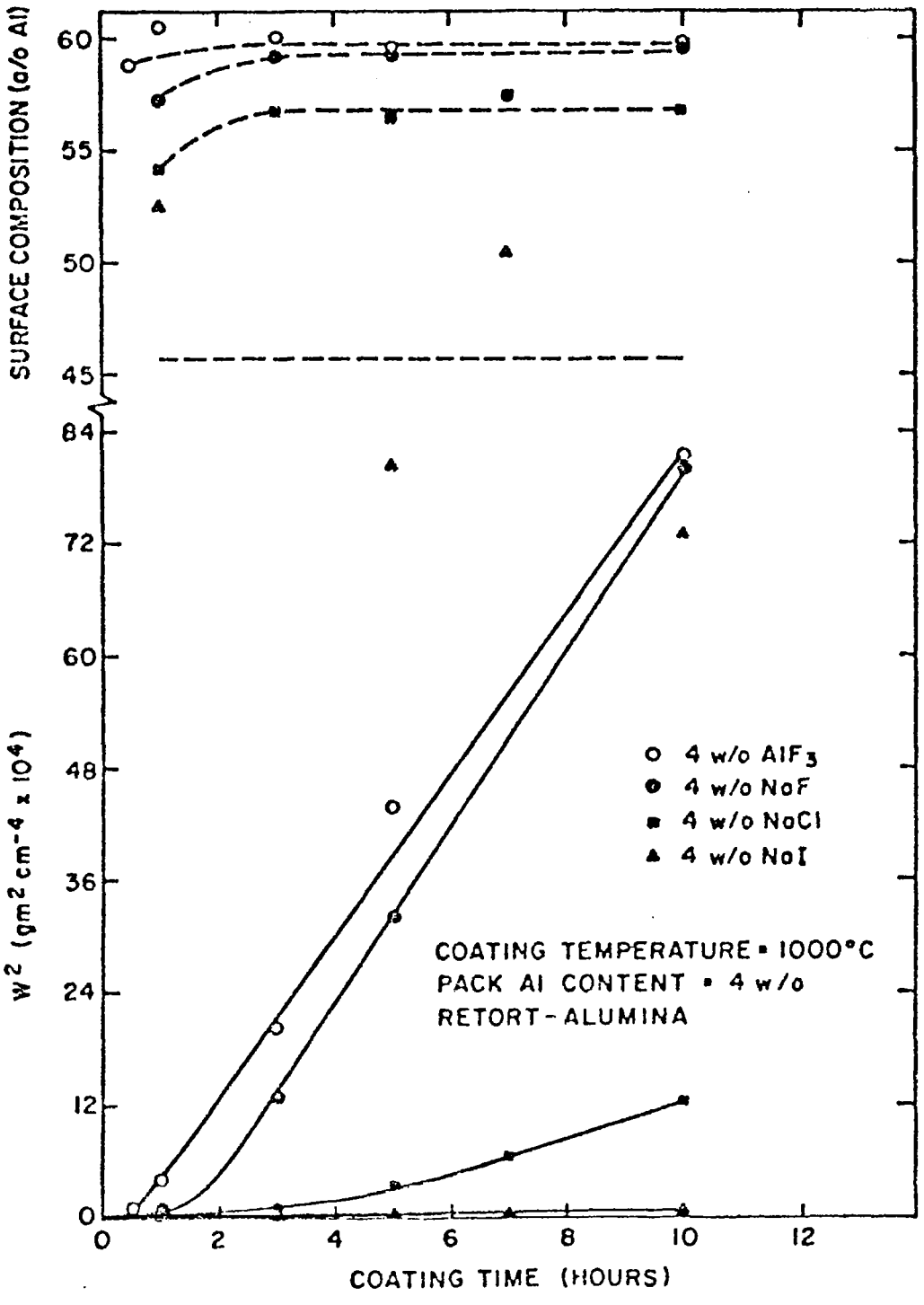

Fig. 11 - Variation of W^2 and Surface Composition With Time in 4 w/o Al Packs at 1000°C.

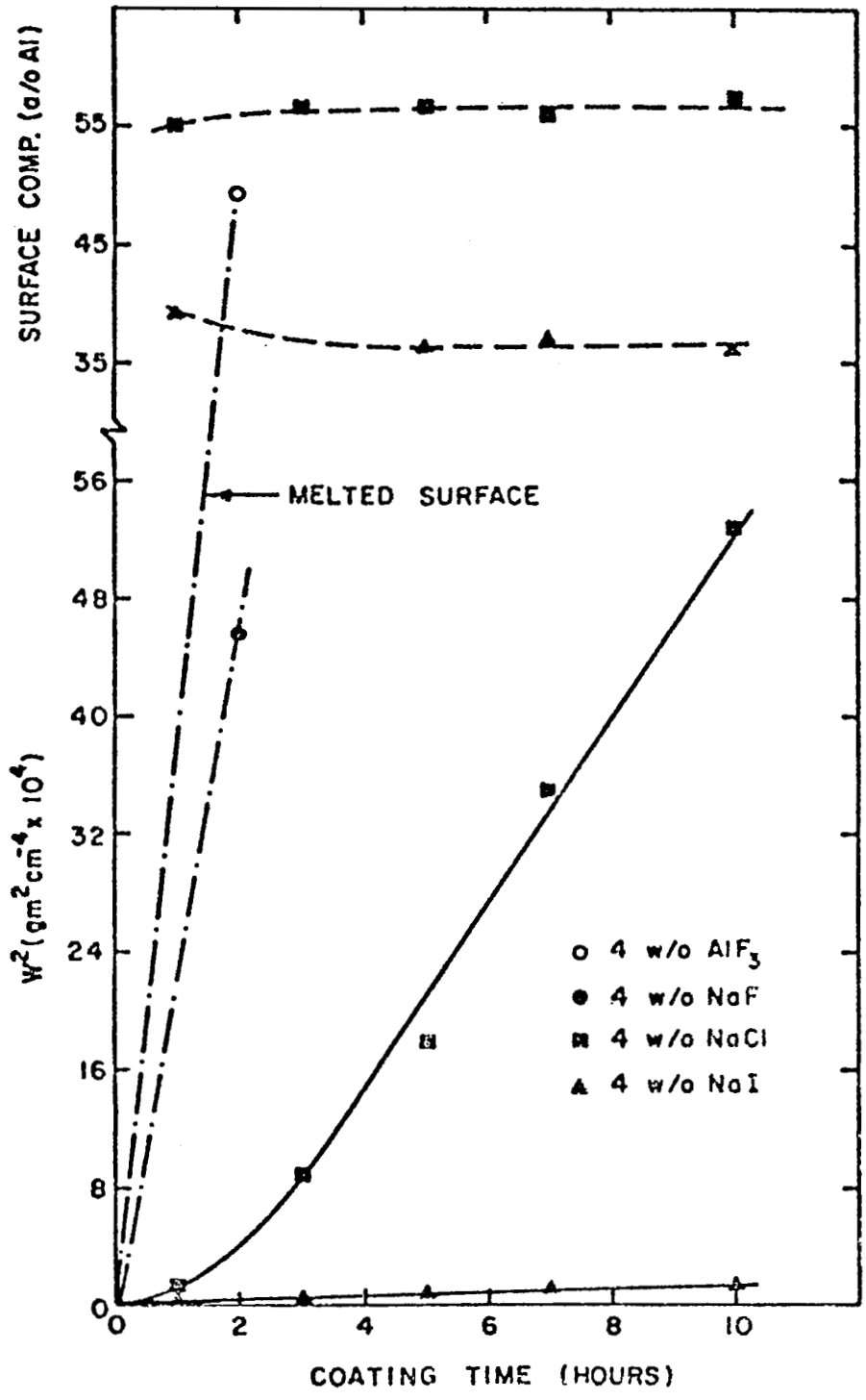

Fig. 12 - Variation of W^2 and Surface Composition With Time in 4 w/o Al Packs at 1093°C.

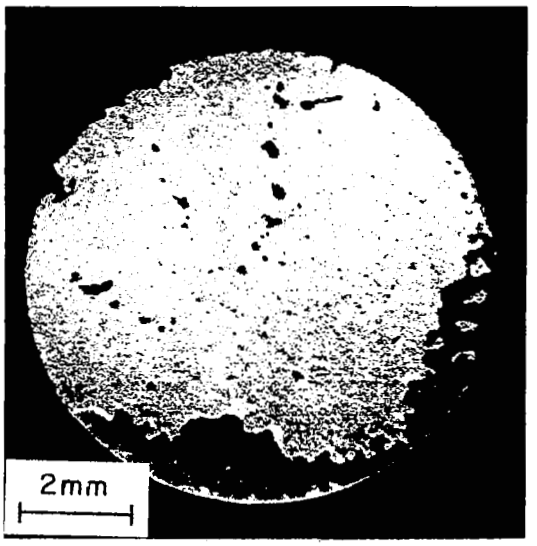

5 Hours

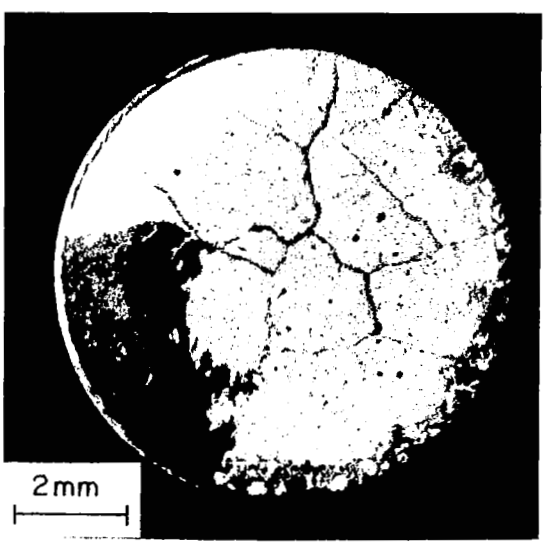

15 Hours

Fig. 13 - Surface Appearance of Specimens Coated in 4 w/o AlF_3 Activated -4 w/o Al Packs at 800°C.

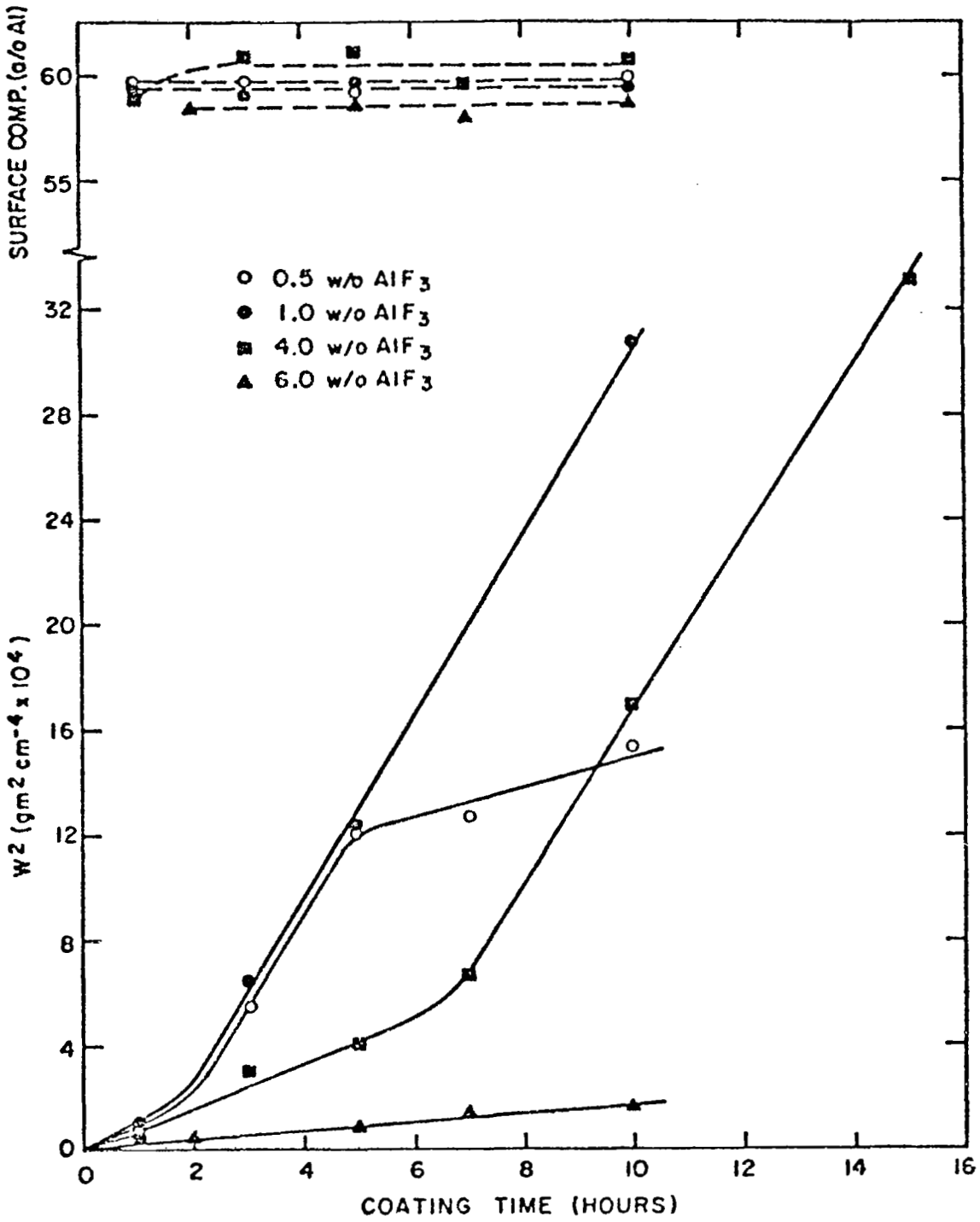

Fig. 14 - Effect of Amount of AlF_3 on W^2 and Surface Composition vs. Time Relationship in 4 w/o Al Packs at 900°C.

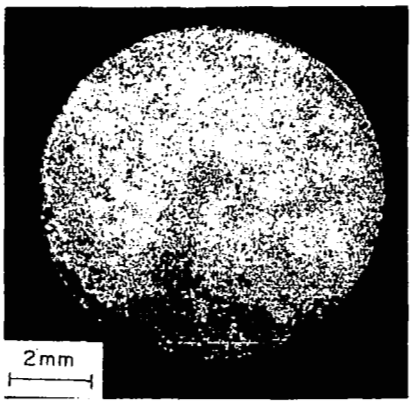

1 w/o AlF_3 - 1 hr.

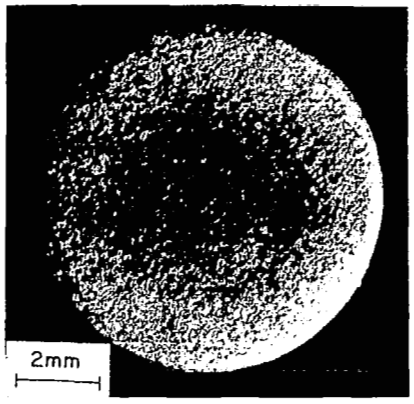

1 w/o AlF_3 - 10 hrs.

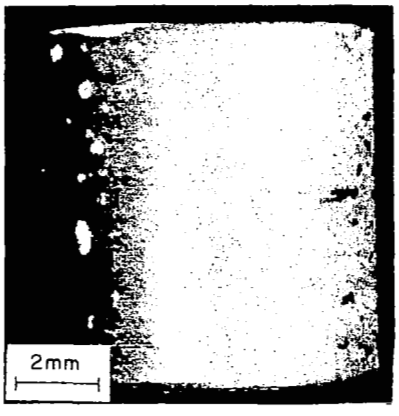

4 w/o AlF_3 - 5 hrs.

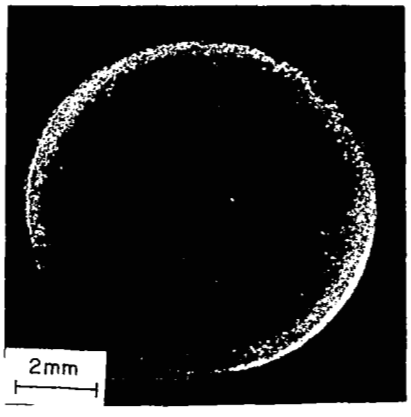

4 w/o AlF_3 - 7 hrs.

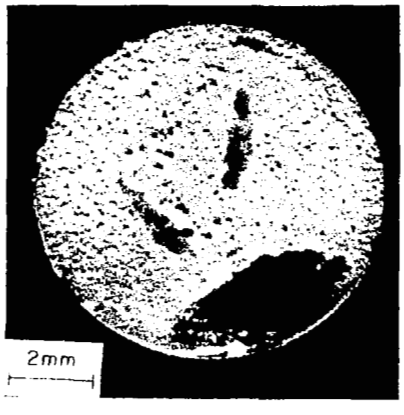

6 w/o AlF_3 - 7 hrs.

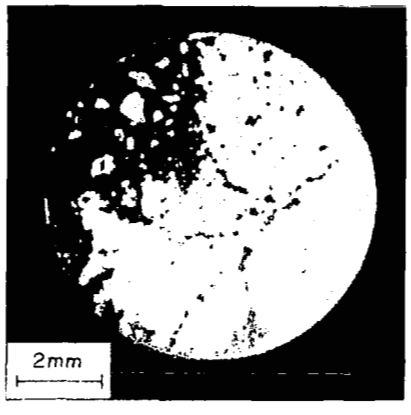

6 w/o AlF_3 - 2 hrs.

Fig. 15 - Surface Appearance of Specimen Coated in 4 w/o AlF_3 activated - 4 w/o Al Pack at 1093°C.

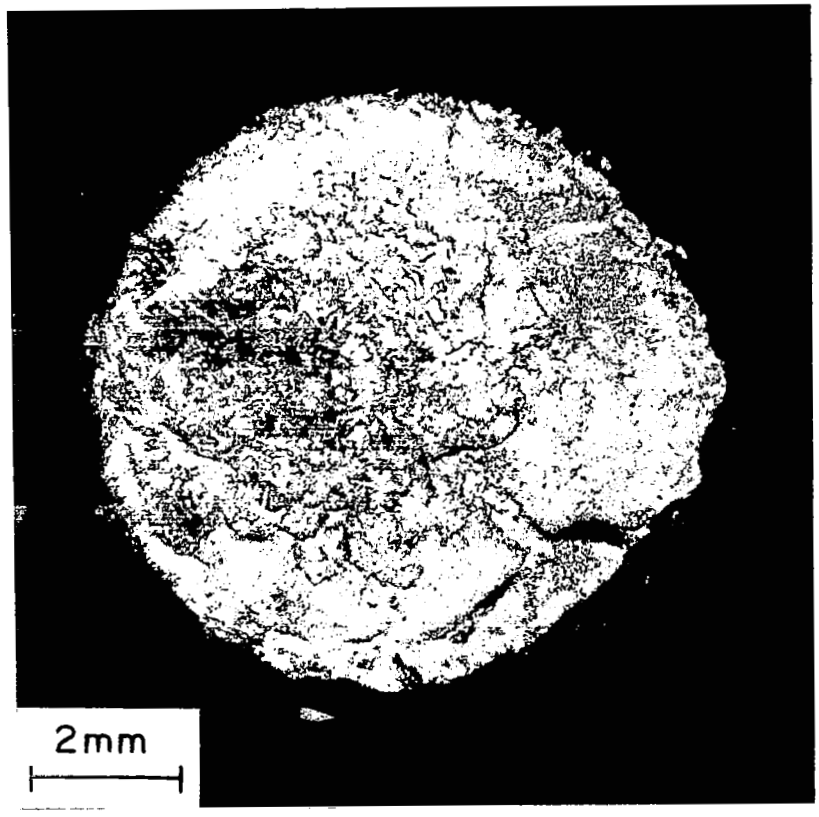

Fig. 16 - Surface Appearance of Specimen Coated in 4 w/o AlF_3 Activated - 4 w/o Al Pack at 1093°C.

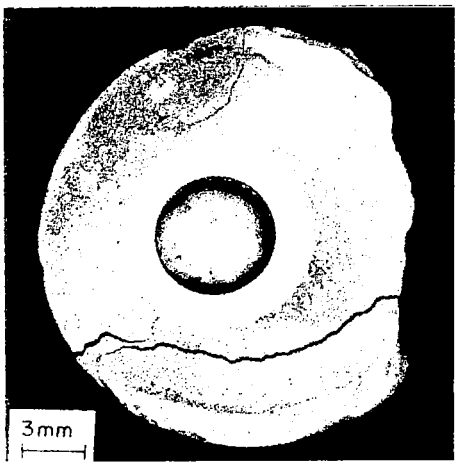

AlF_3

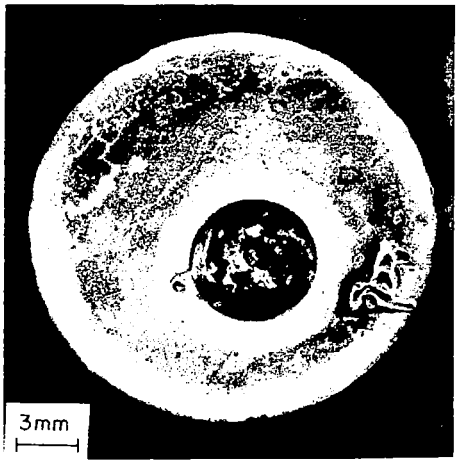

NaF

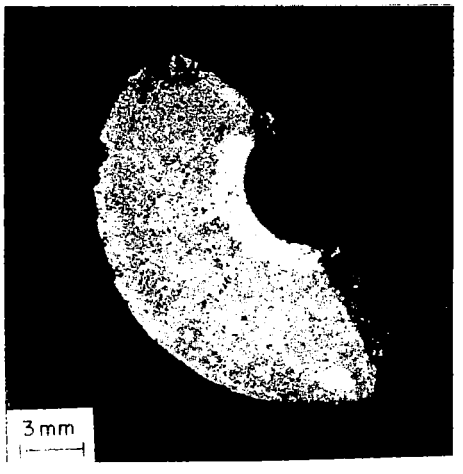

NaCl

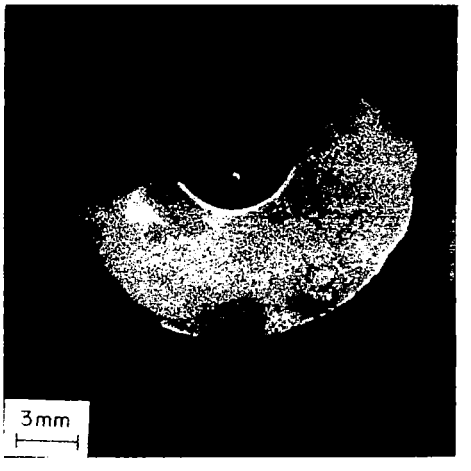

NaI

Fig. 17 - Appearance of Depleted Zones in 4 w/o Al Packs after Coating for 10 hrs. at 1000°C.

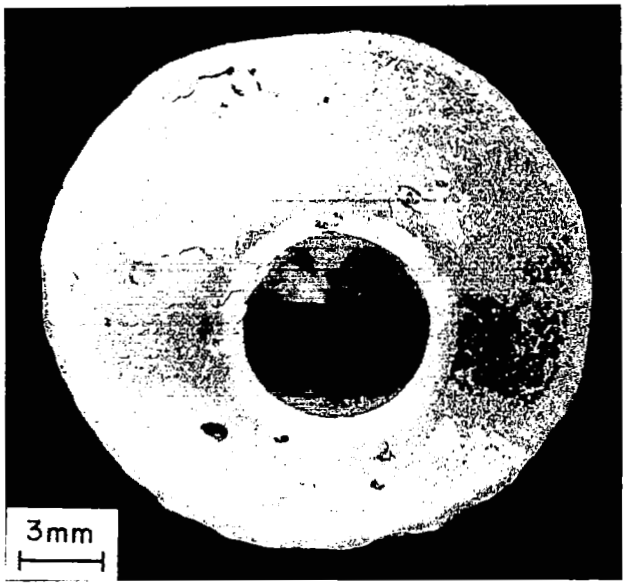

A

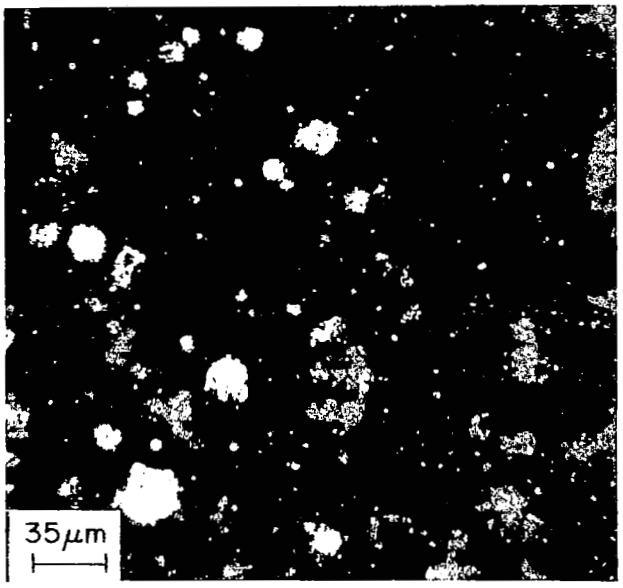

B

Fig. 18 - Appearance of Depleted Zone in 4 w/o AlF_3 Activated - 4 w/o Al Pack After Coating at 1093°C.

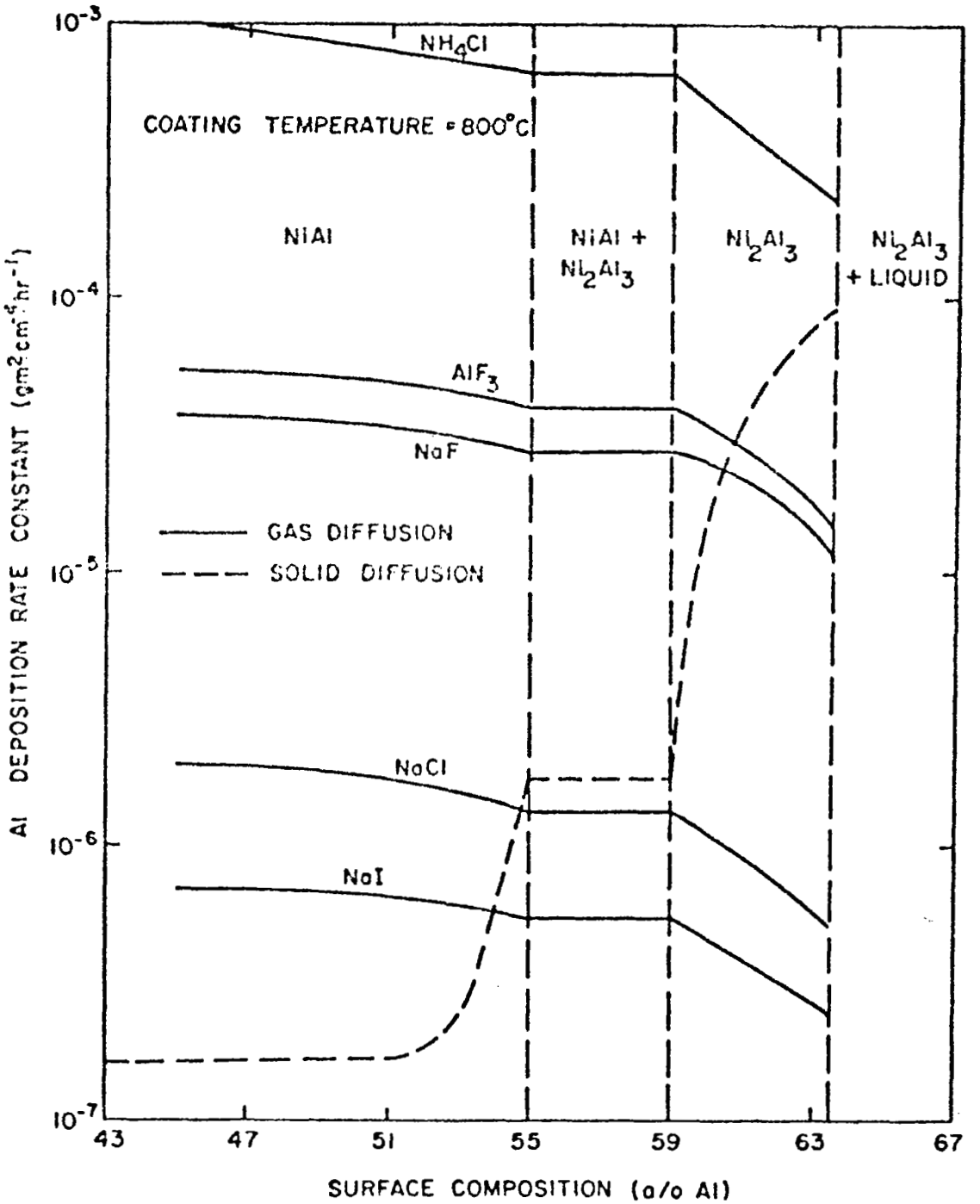

Fig. 19 - Variation of K_g and K_s with Surface Composition in 4 w/o Al Packs at 800°C.

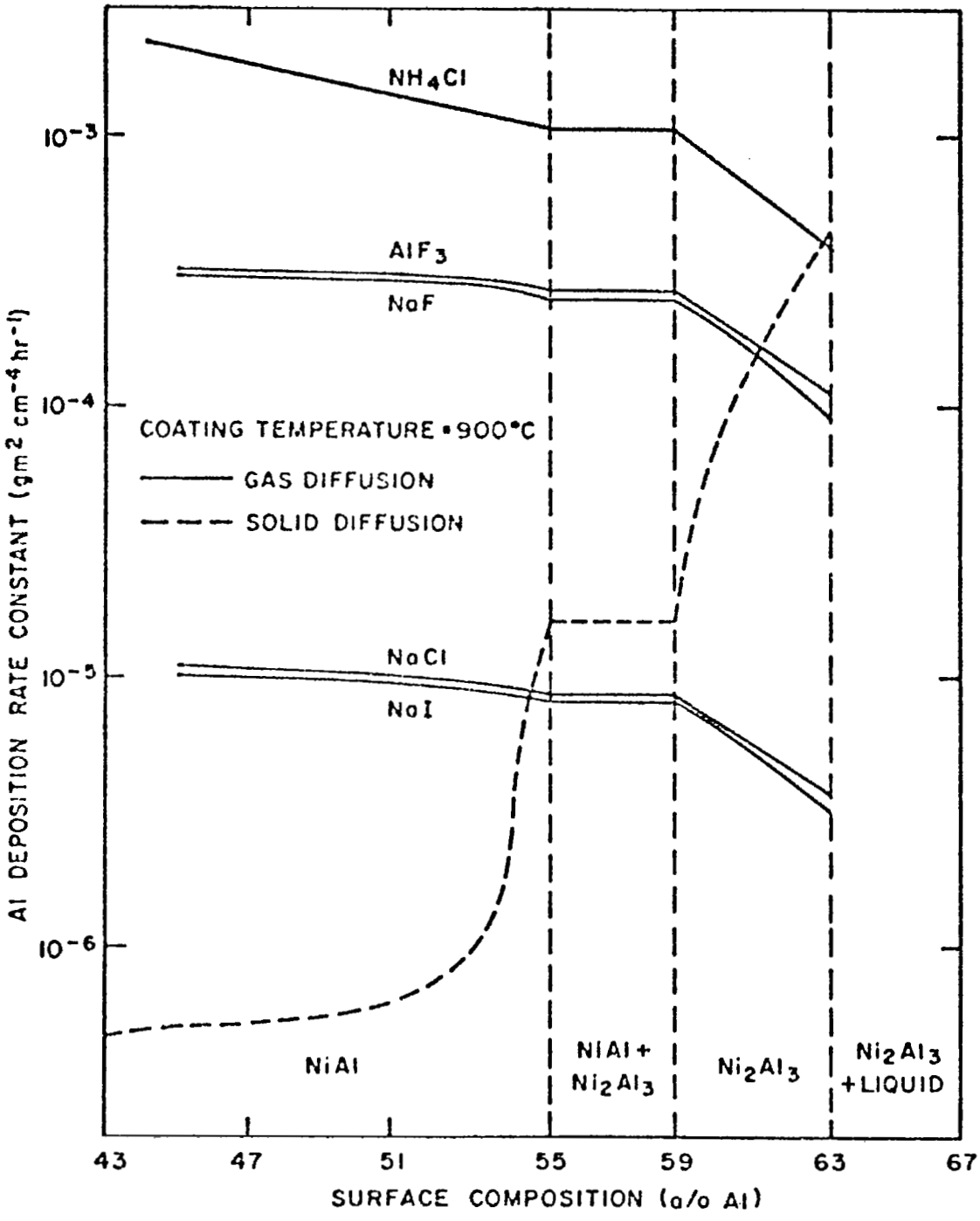

Fig. 20 - Variation of K_g and K_s with Surface Composition in 4 w/o Al Packs at 900°C.

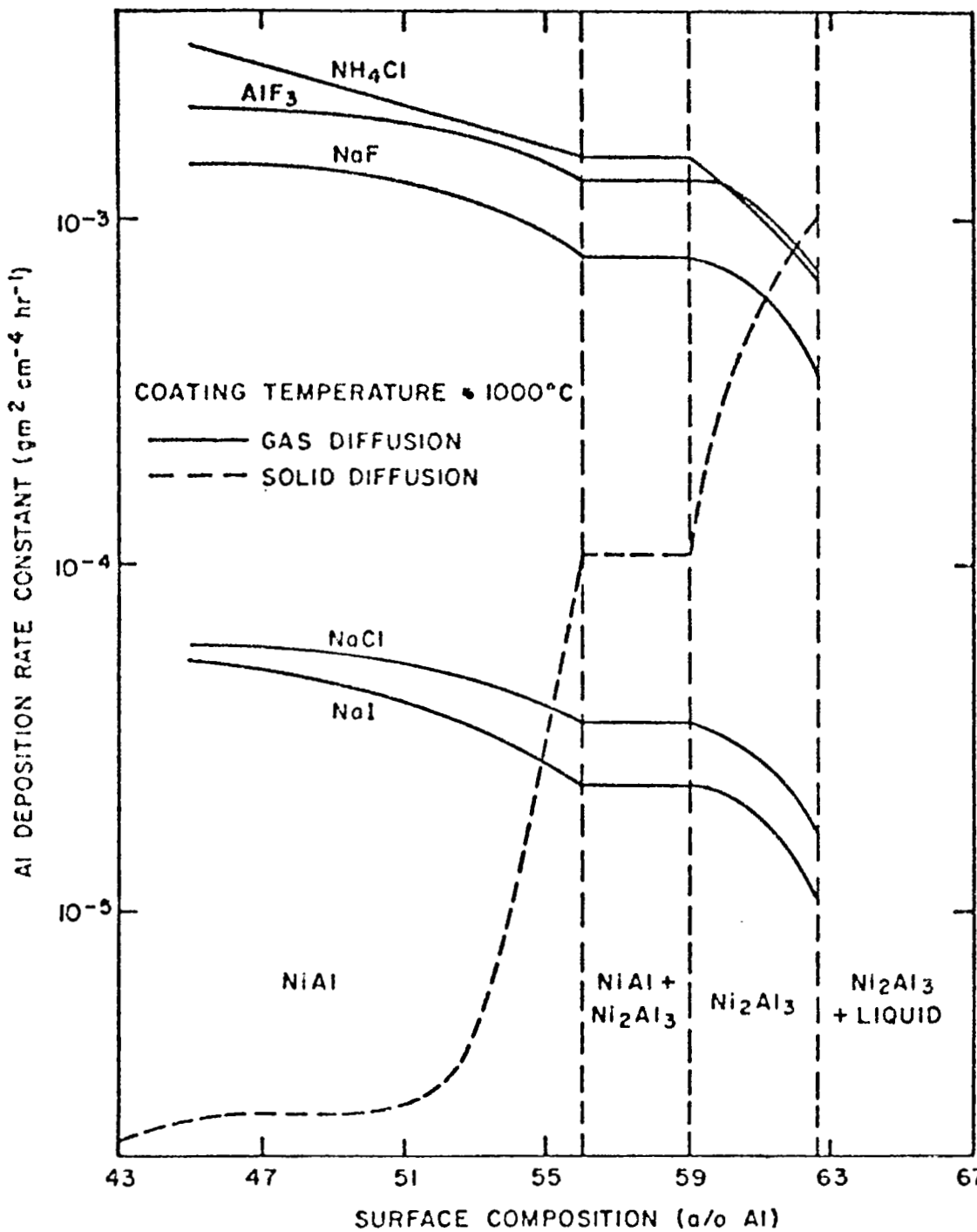

Fig. 21 - Variation of K_g and K_s with Surface Composition in 4 w/o Al Packs at 1000°C.

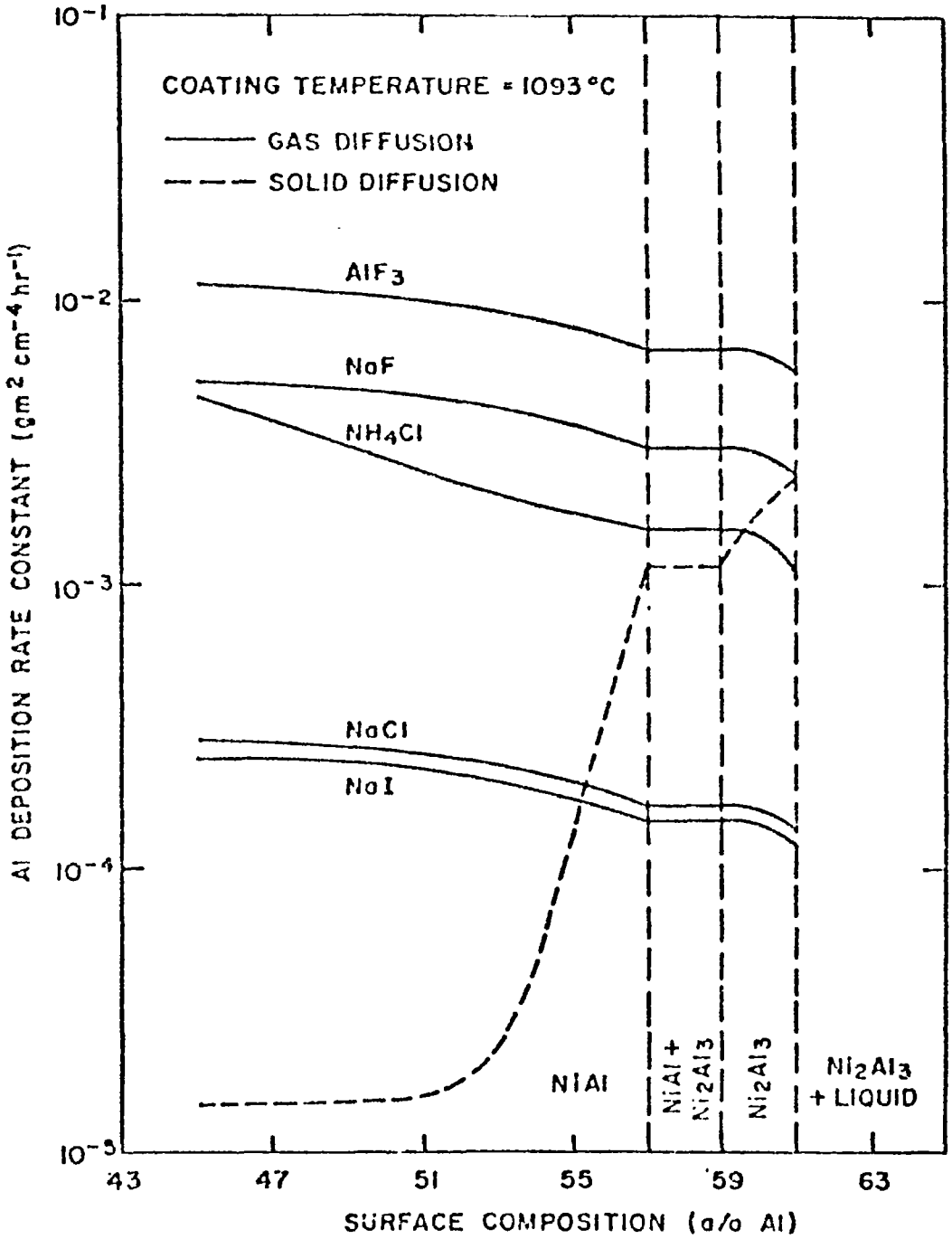

Fig. 22 - Variation of K_g and K_s with Surface Composition in 4 w/o Al Packs at 1093°C.

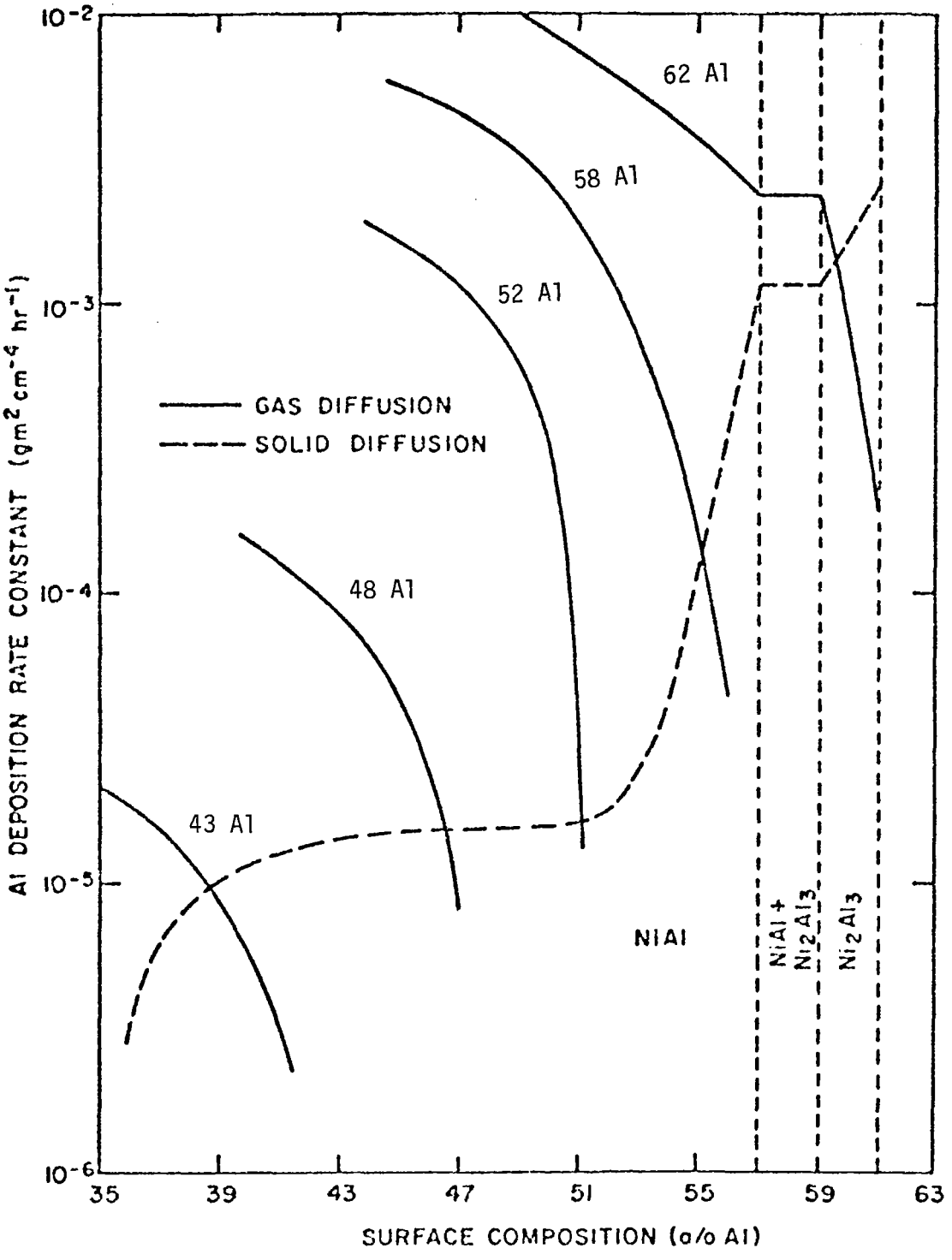

Fig. 23 - Variation of K_g and K_s with Surface Composition in 4 w/o AlF_3 Activated Alloy Packs at 1093°C.

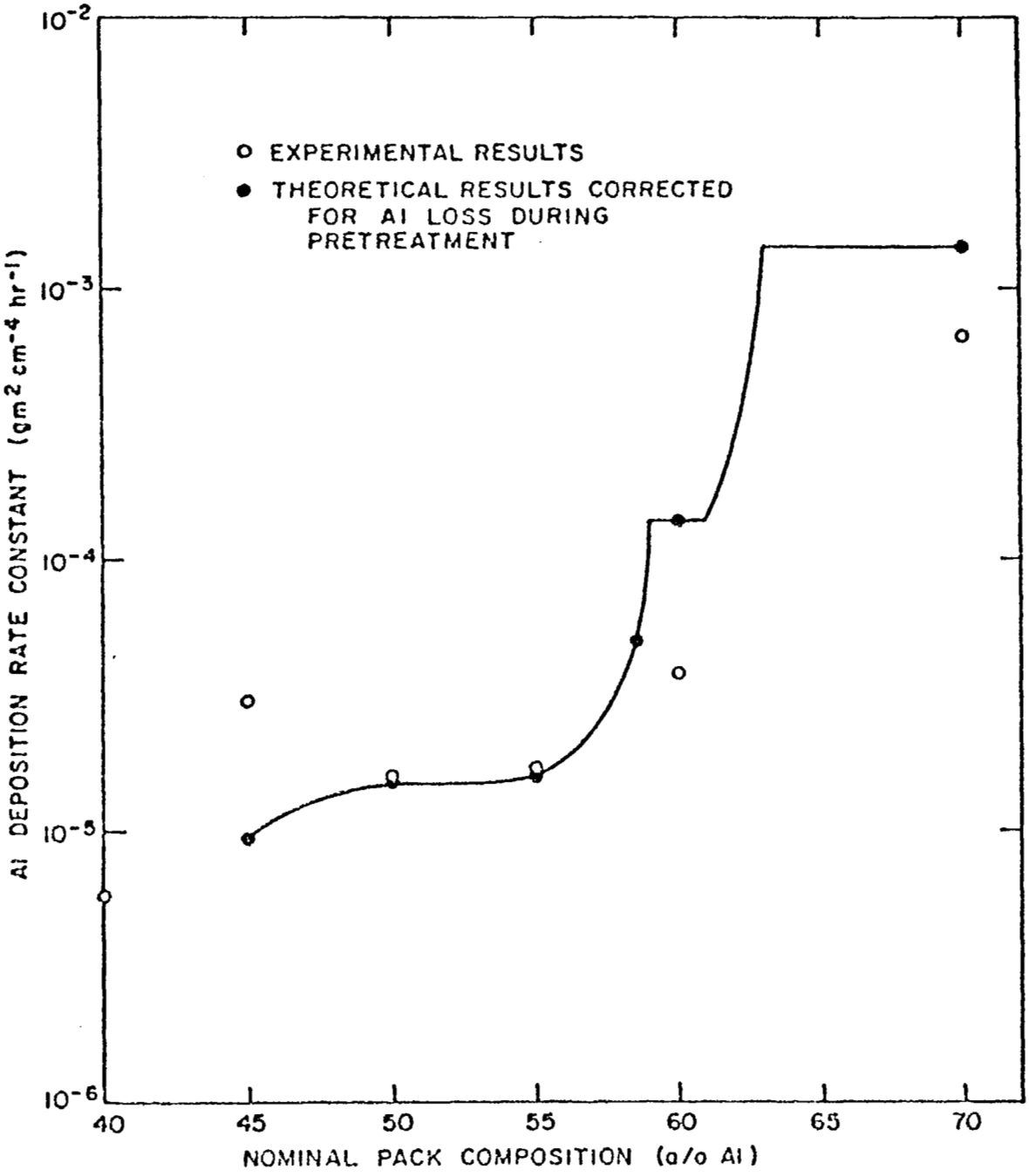

Fig. 24 - Comparison of Theoretical and Observed Rate Constants for 4 w/o AlF_3 Activated Alloy Packs at 1093°C.

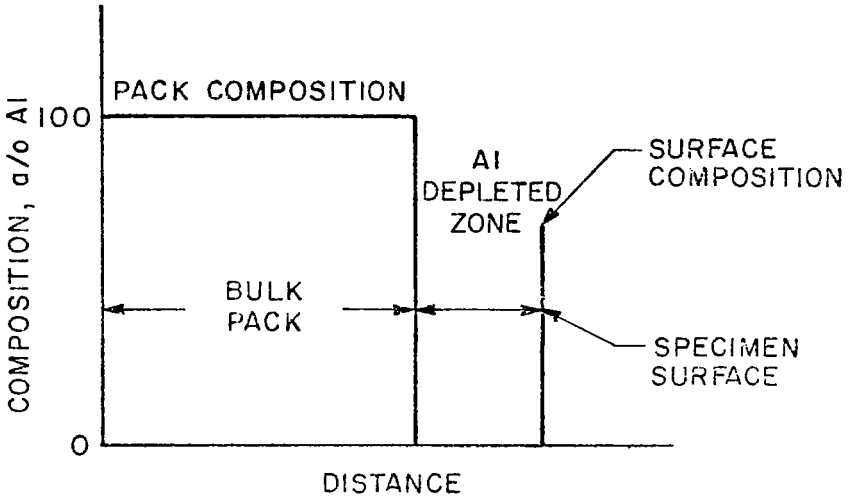

PURE Al PACK

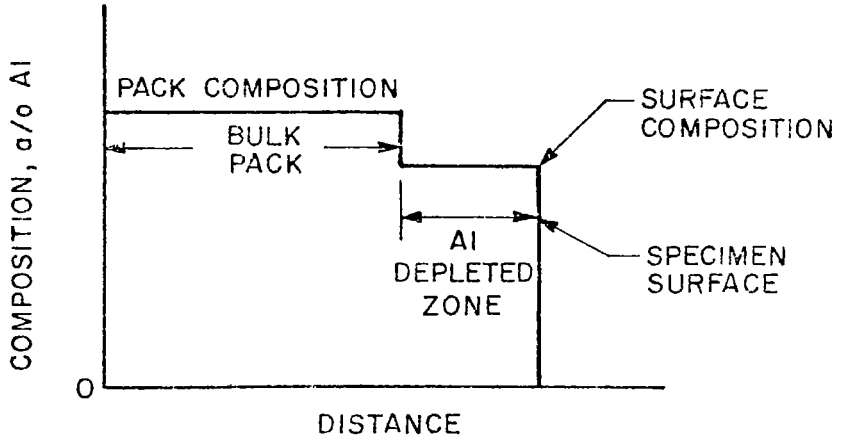

Ni-Al ALLOY PACK

Fig. 25 - Schematic Concentration Profiles in Pure Al and Alloy Packs

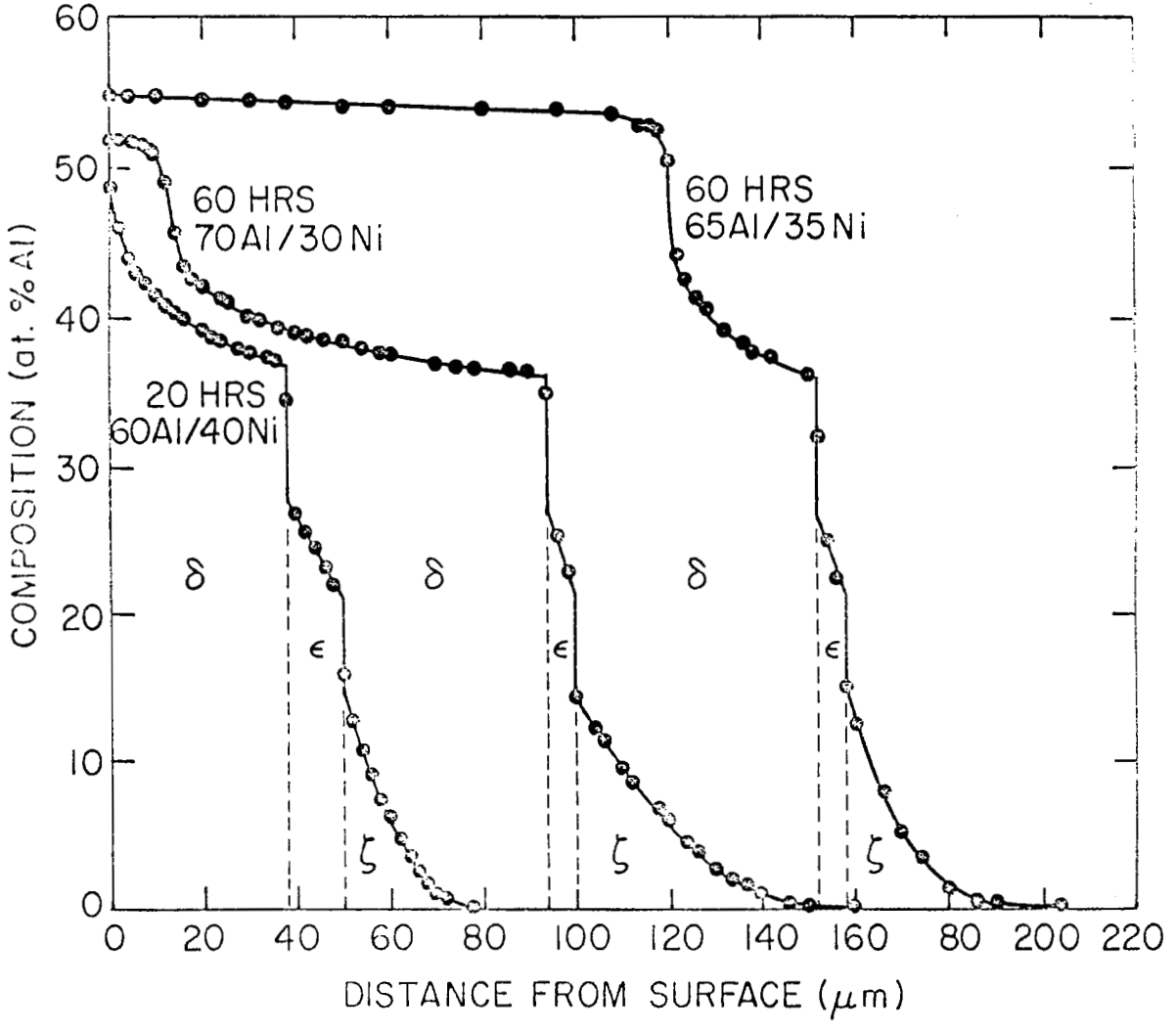

Fig. 26 - Effect of Pack Al/Ni Ratio on Concentration Profile at 1000°C.

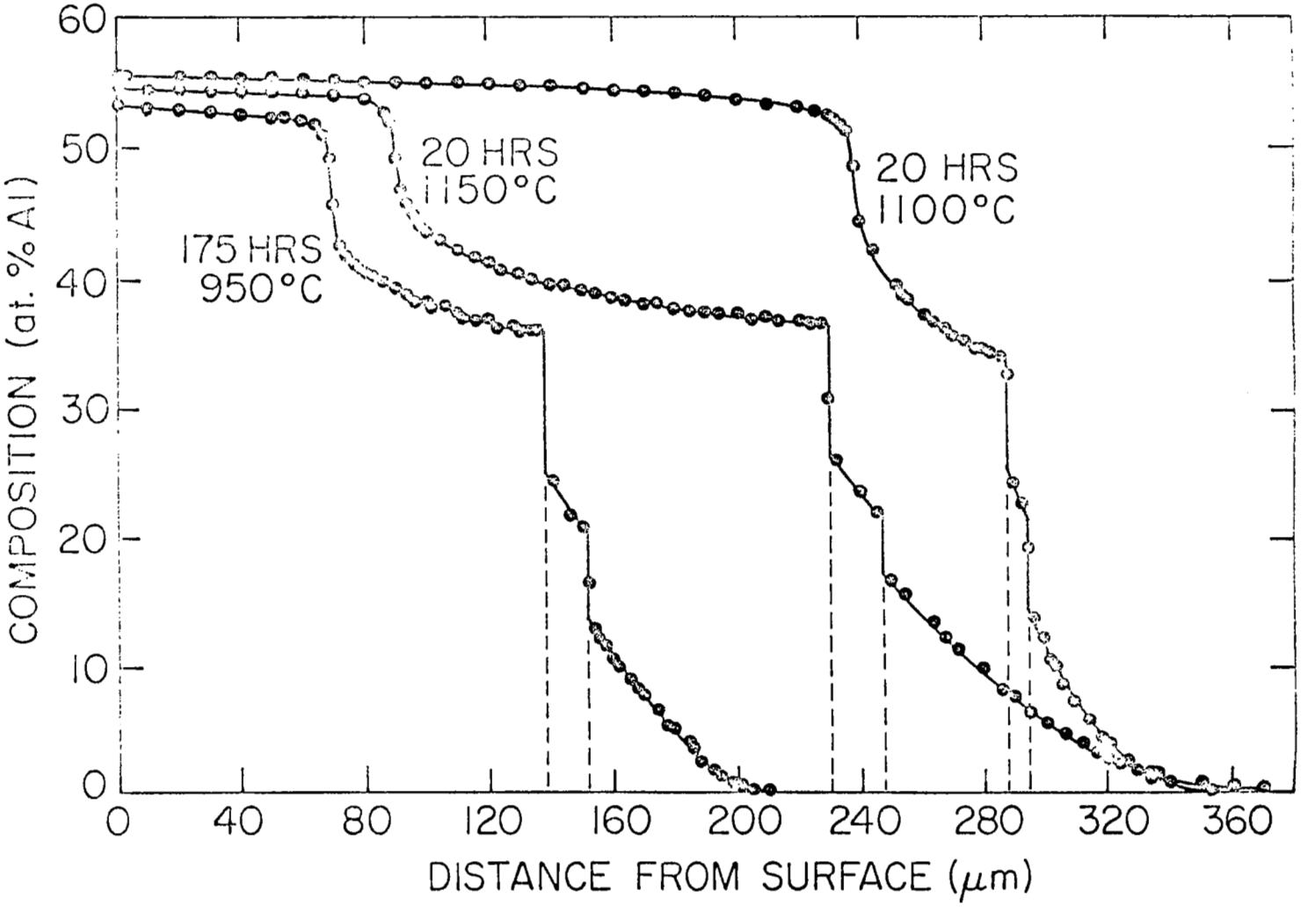

Fig. 27 - Effect of Temperature on Concentration Profile in 70 Al/30 Ni Pack.

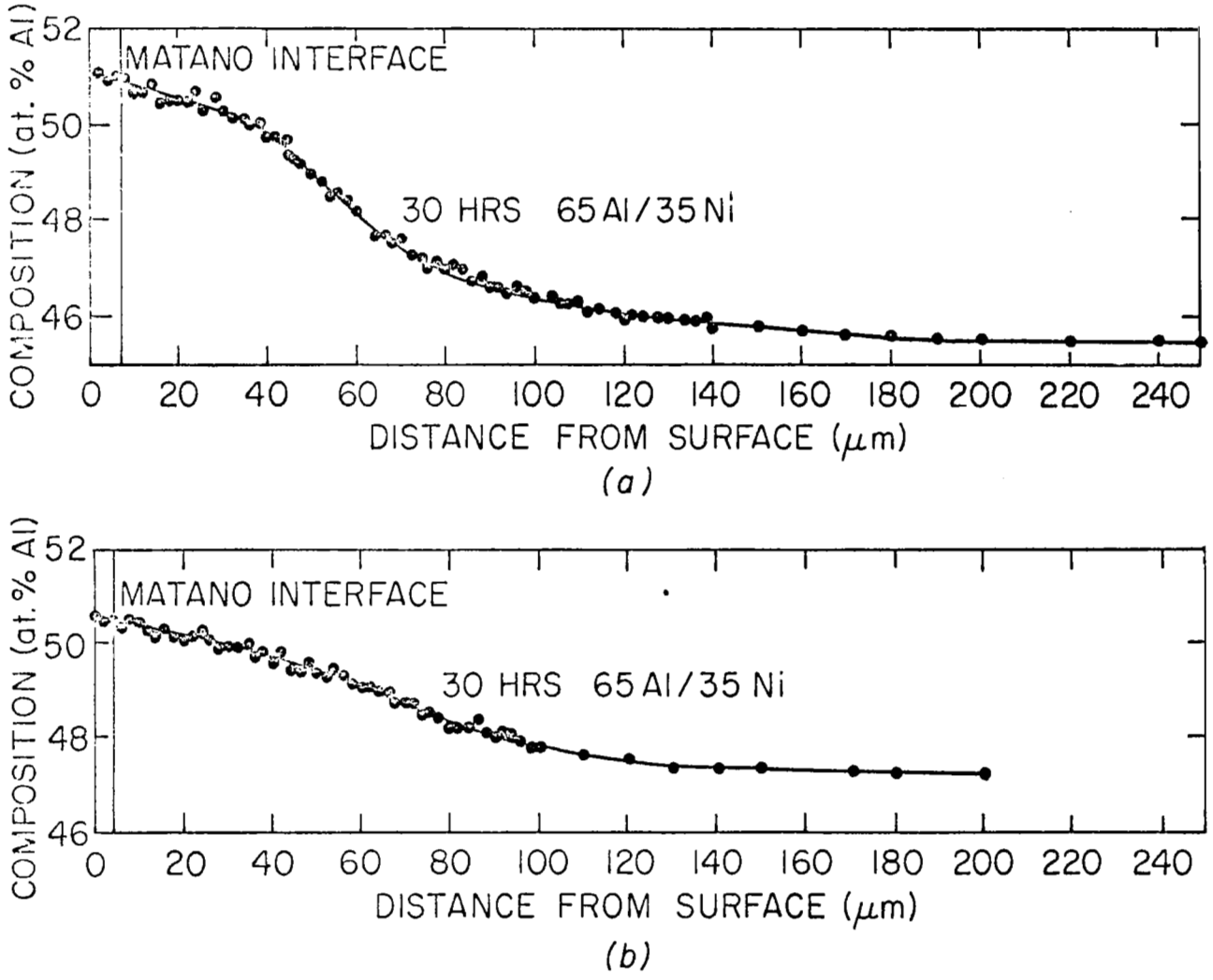

Fig. 28 - Concentration Profiles in NiAl Specimens at 1150°C.

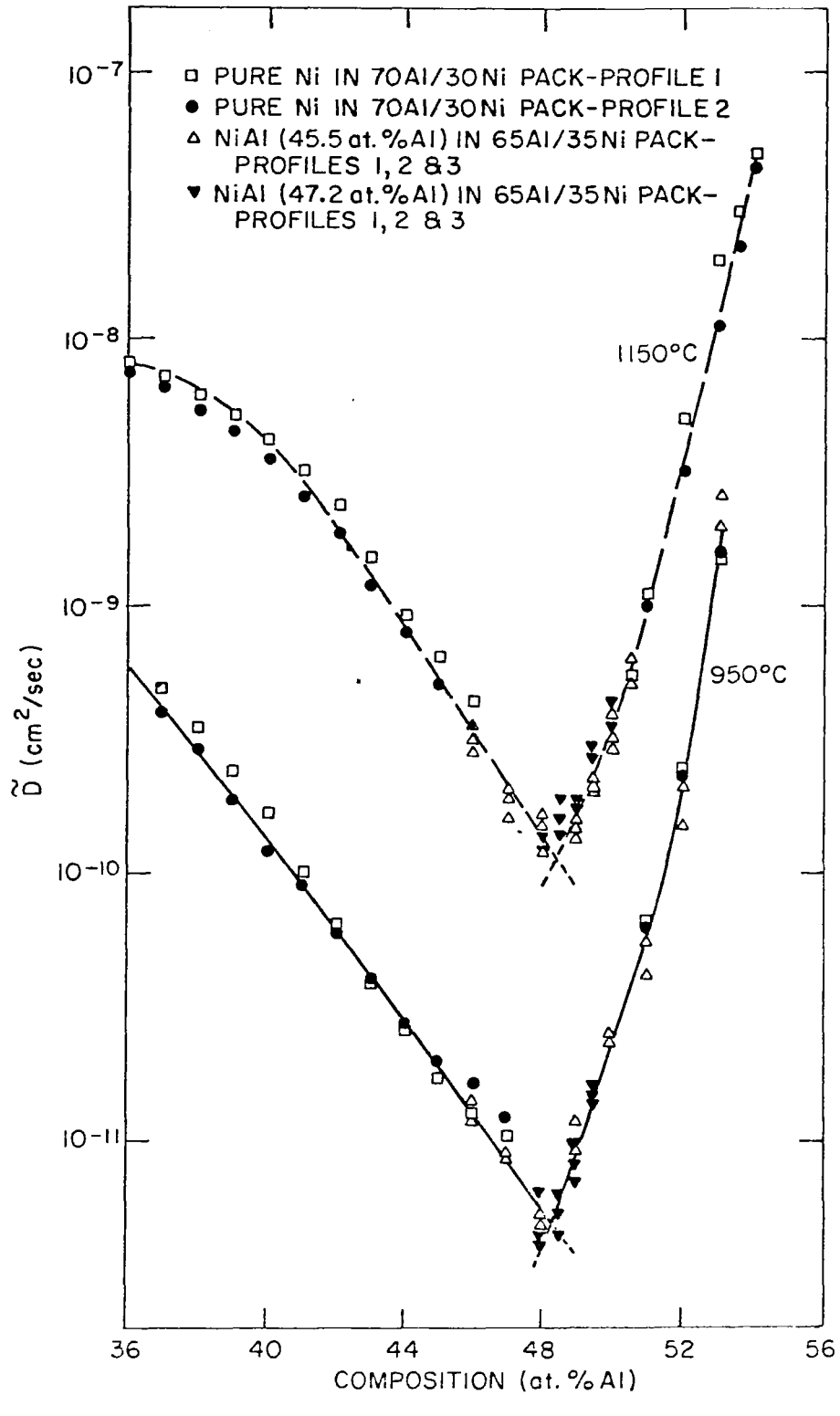

Fig. 29 - Variation of D_{δ} with Composition at 950 and 1150°C.

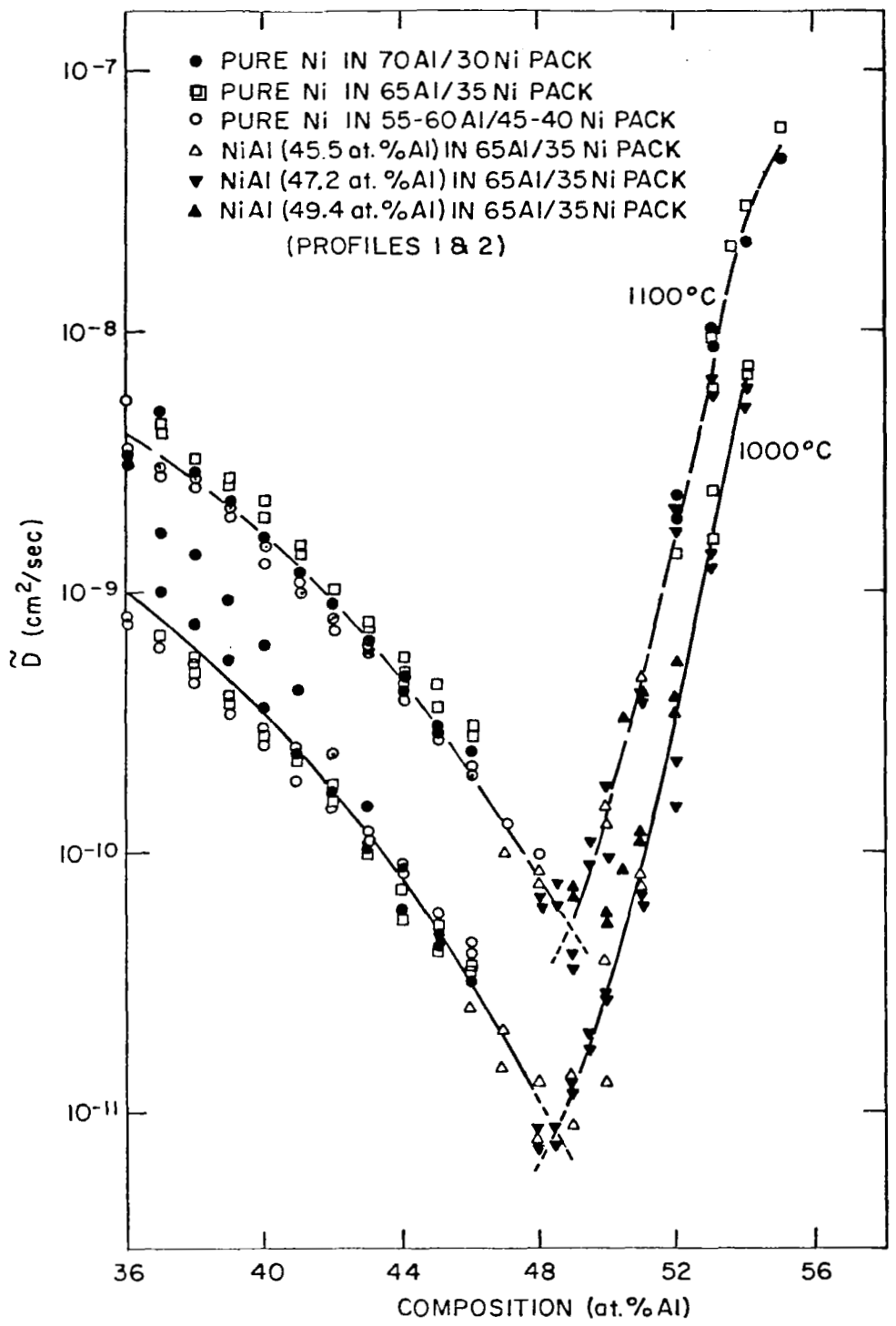

Fig. 30 - Variation of D_δ with Composition at 1000 and 1100°C.

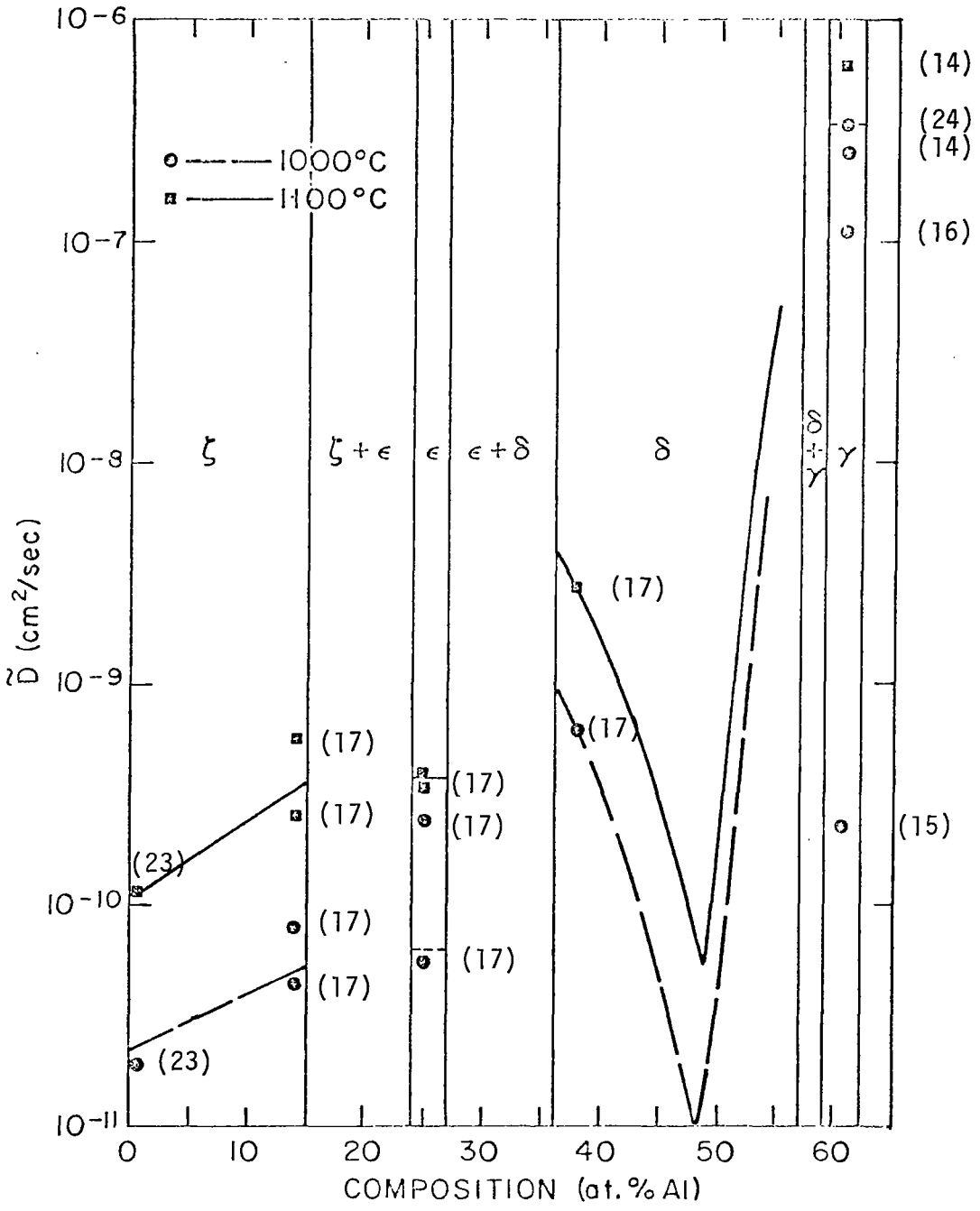

Fig. 31 - Interdiffusion Coefficients in the Al-Ni System

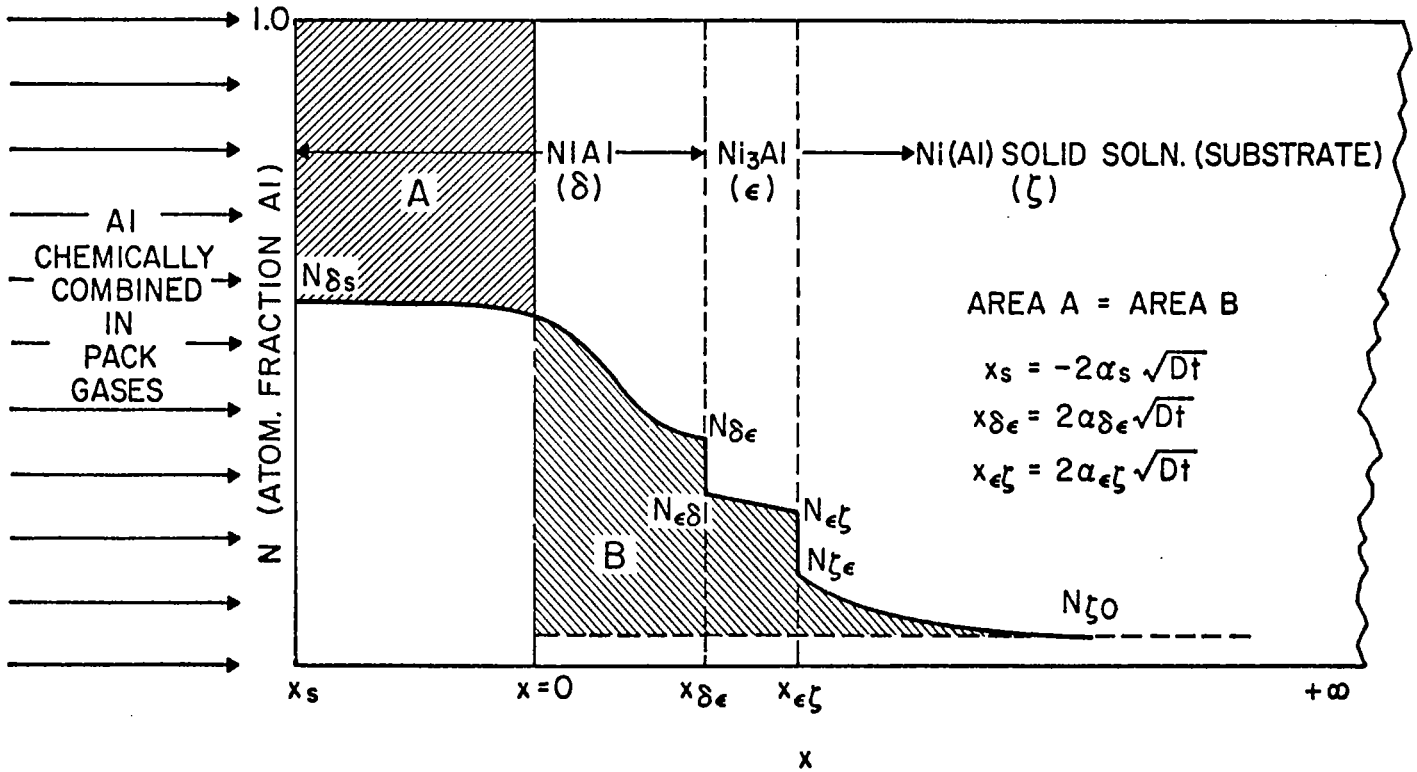

Fig. 32 - Schematic Diagram of Concentration Profile of Aluminide Coating on Ni.

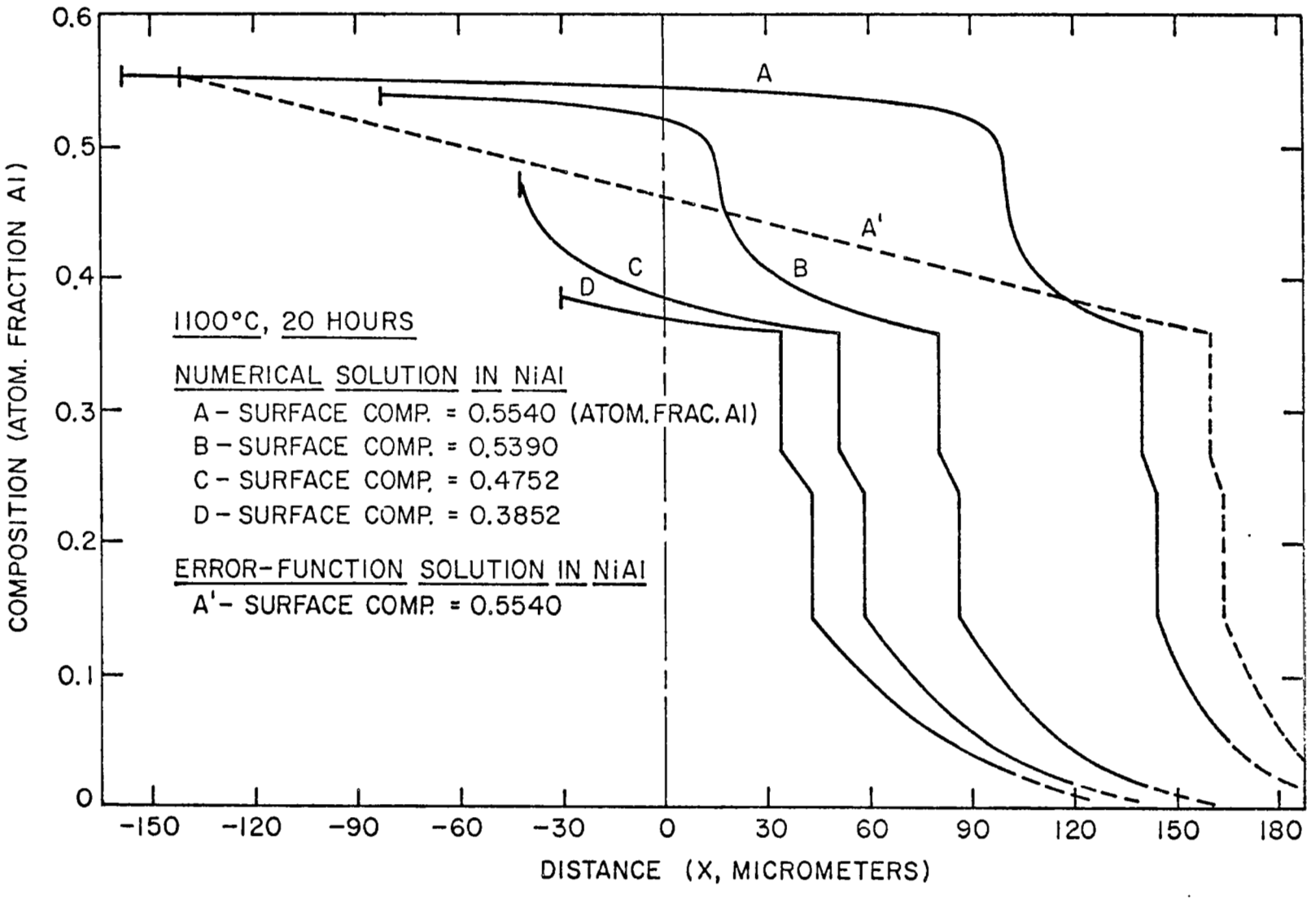

Fig. 33 - Calculated Composition Profiles for Aluminization at 1100°C for 20 hrs.

1. Report No.	2. Government Accession No.	3. Recipient's Catalog No.
NASA CR-2939		

4. Title and Subtitle	5. Report Date
KINETICS OF PACK ALUMINIZATION OF NICKEL	January 1978
	6. Performing Organization Code
7. Author(s)	8. Performing Organization Report No.
L. L. Seigle, B. K. Gupta, R. Shankar, and A. K. Sarkhel	None
	10. Work Unit No.
9. Performing Organization Name and Address	
State University of New York Stony Brook, New York 11794	11. Contract or Grant No. NGR-33-015-160
	13. Type of Report and Period Covered
12. Sponsoring Agency Name and Address	Contractor Report
National Aeronautics and Space Administration Washington, D.C. 20546	14. Sponsoring Agency Code

15. Supplementary Notes

Final report. Project Manager, Stanley R. Levine, Propulsion Laboratory, U.S. Army R&T Laboratories (AVRADCOM), NASA Lewis Research Center, Cleveland, Ohio 44135

16. Abstract

A study has been made of the kinetics of pack aluminization of unalloyed nickel in packs of varying aluminum activity with various halide activators. Surface compositions of the coatings as functions of time, temperature, and pack composition were obtained in order to establish the boundary conditions for diffusion in the system. The structure of the packs was also examined in order to clarify the mechanism of aluminum transport. The results indicate that the kinetics of pack aluminization are controlled jointly by gas diffusion in the pack and solid diffusion in the coating. Levine and Caves' model for gas diffusion was combined with calculations of rates of diffusion in the solid to formulate a more complete theory for the kinetics of pack aluminization.

17. Key Words (Suggested by Author(s))	18. Distribution Statement
Aluminide coatings Pack aluminization Protective coatings	Unclassified - unlimited STAR Category 26

19. Security Classif. (of this report)	20. Security Classif. (of this page)	21. No. of Pages	22. Price*
Unclassified	Unclassified	73	A04

* For sale by the National Technical Information Service, Springfield, Virginia 22161

NASA-Langley, 1978